PETROGENESIS OF KREEP

G. A. McKAY and D. F. WEILL

Department of Geology, University of Oregon, Eugene, Oregon 97403

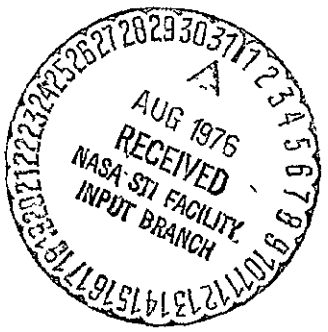

ABSTRACT

Solid/liquid distribution coefficients (weight basis) have been experimentally determined for a number of trace elements for olivine, orthopyroxene, plagioclase and ilmenite. Values of distribution coefficients measured at 1200°C and f_{O_2} of $10^{-13.0}$ for liquids similar in composition to the olivine-opx-plagioclase peritectic in the pseudoternary system $(Fe,Mg)_2SiO_4$-$CaAl_2Si_2O_8$-SiO_2 are as follows: olivine; Ce = 0.010 ±.007, Sm = 0.015 ±.005, Eu = 0.015 ±.005, Yb = 0.033 ±.002, Cr = 1.2 ±.1: orthopyroxene; Ba = 0.011 ±.005, Cr = 5.2 ±.2: anorthite; Rb = 0.017 ±.008, Ba = 0.15 ±.03. Values measured at 1140°C and f_{O_2} of $10^{-12.8}$ for liquids similar in composition to high-Ti mare basalts are as follows: ilmenite; Ce = 0.006 ±.003, Sm = 0.010 ±.002, Eu = 0.007 ±.003, Yb = 0.075 ±.005. Cr distribution coefficients decrease with decreasing oxygen fugacity for both pyroxene and olivine, but are larger for pyroxene than for olivine at all fugacities investigated. The variation of D^{Cr} with oxygen fugacity indicates that a substantial fraction of the Cr is divalent at lunar oxygen fugacities.

Major and trace element partitioning and relevant phase equilibria are used to investigate possible parent-daughter relationships between a number of highland samples and highly evolved KREEP-rich materials. Out of about 80 highland samples tested, 33 are found to be possible parents to the KREEP-rich materials. The average composition of these 33 samples is very similar to that of the Low-K Fra Mauro basalt (LKFM). A model is proposed in which LKFM-type material was produced by fractionation of large amounts of olivine and lesser amounts of plagioclase (and possibly other minor phases) from undifferentiated lunar material at ∿ 4.4 AE. During the same episode of igneous activity, some LKFM material differentiated to form a series of more evolved members of the KREEP suite, including material of

peritectic bulk composition in the $(Mg,Fe)_2SiO_4$-$CaAl_2Si_2O_8$-SiO_2 pseudoternary system. In a later igneous event at ∿ 3.9 AE, some of this peritectic material further differentiated, producing more highly evolved KREEP such as sample 15386. The model is consistent with phase equilibria, major and trace element partitioning, and Rb-Sr isotopic data.

INTRODUCTION

There is a large family of lunar highland rocks with marked enrichment in a number of minor and trace elements (K, P and the rare earth elements, among others) which are not readily incorporated into the crystal lattices of the major rock-forming minerals. These KREEP-rich highland rocks are also characterized by bulk compositions which, when plotted in the $(Mg,Fe)_2SiO_4$-SiO_2-$CaAl_2Si_2O_8$ pseudoternary liquidus diagram, form a continuum extending along the olivine-plagioclase cotectic line through the olivine-plagioclase-pyroxene peritectic point and along the plagioclase-pyroxene cotectic line (Fig. 1 and Table 1). A few of these rocks, such as 15386, have igneous textures. Most of them are breccias, and many of these are polymict. Most KREEP-rich samples are therefore mechanical mixtures of fragments of rocks or minerals. As such, they could be considered mixtures of the "essence of KREEP" or the "KREEP component" with other lunar rock types such that the high overall concentration and the relative abundances of K, REE, P and associated "incompatible" elements are dominated by the KREEP component, while the bulk composition is determined by the relative proportions of all the lunar rock types in the mixture. According to this point of view differences in the major element composition of KREEP-rich samples are primarily determined by a variable history of mechanical mixing.

Other interpretations are possible. Walker et al. (1972) pointed out that the major element compositions of the KREEP-rich rocks cluster along solid-liquid saturation curves of the pseudoternary phase diagram, suggesting that they had evolved as a result of liquid separations from equilibrated partially molten phase assemblages within the pseudoternary system. In approaching the problem of KREEP we assume that the association of their bulk chemistry with liquid saturation

boundaries is not coincidental. Therefore, even though these rocks have been subjected to impact fragmentation, recombination and thermal metamorphic effects on the lunar surface we take the view that their bulk compositions have not been greatly altered and that the general characteristics of their chemical compositions can be interpreted mainly in terms of equilibrium crystallization and melting.

It is consistent with the major element compositions of all these rocks that they are related by the solid-liquid phase equilibria depicted in Fig. 1. Therefore, it is logical to ask whether such relationships are also compatible with the trace element chemical data. Using the phase equilibria in Fig. 1 and the solid/liquid distribution coefficients for a number of key elements it is possible to relate the proportions of solid and liquid during differentiation to the resulting trace element fractionation trends. Conversely, given the trace element concentrations in an assumed parent assemblage and its derivative, we can calculate the proportions of the major phases involved in the fractionation process and check for compatibility with the phase diagram. Using the above approach Weill and McKay (1975) demonstrated that it is improbable that the KREEP-rich rocks were derived by igneous fractionation from what is now estimated to be the average highlands composition (Taylor and Jakeš, 1974). Weill and McKay (1975) also investigated the possibility of deriving KREEP liquids by one-step equilibrium partial melting or crystallization of compositions similar to those proposed for the whole moon (Ganapathy and Anders, 1974; Taylor and Jakeš, 1974). It was concluded that such an origin is consistent with the known constraints of phase equilibria and trace element distribution behavior if a few percent or less of KREEP liquid had equilibrated with a mineral assemblage of olivine, Ca-poor pyroxene and plagioclase.

We believe these conclusions are still valid, but the resulting model for the origin of KREEP-rich rocks is not unique or complete. Our previous calculations addressed themselves to the derivation of KREEP-rich compositions corresponding

closely to the pseudoternary peritectic and did not attempt to investigate the possible relationships among the total range of KREEP-rich rocks. Perhaps a multiple-step origin is equally plausible (e.g., recent Sm/Nd isotopic data presented by Lugmair et al. (1976) indicate a minimum of two steps for the origin of KREEP sample 15382). Hence, it is appropriate in this paper to consider the possibility of multiple-step derivation of KREEP and the relationships between the KREEP-rich compositions generated at successive stages of evolution. In this context we also discuss the effect of the igneous processes involved in the evolution of KREEP on Rb-Sr isotopes. Finally, we also present some recent experimental determinations of solid/liquid distribution coefficients for the REE in olivine and ilmenite and Cr, Ba and Rb in plagioclase and pyroxene.

EXPERIMENTAL METHODS

A set of bulk compositions were prepared so that when they were held at 1200°C and at oxygen fugacities low enough to maintain the Fe predominantly in the divalent state they produced several percent of either olivine, orthopyroxene or plagioclase in equilibrium with liquids of compositions close to the peritectic point in Fig. 1. These bulk compositions were then enriched with an additional 1-3 wt % of one of the large-ion-lithophile elements (or about 0.5 wt % in the case of Cr) and held at temperature and oxygen fugacity (H_2/CO_2 mixing) in SiC resistance furnaces for 50-150 hours before quenching. Ilmenite/liquid distribution coefficients were determined in bulk systems corresponding to high-Ti mare basalts with 1-3 wt % LIL element added. In order to minimize Fe losses during runs the charges were held in PtRh wire loops which had previously been held in contact with similar compositions at T and f_{O_2} similar to run conditions. After quenching, crystals and glass were analyzed by electron probe. The distribution coefficients and the details of phase compositions for these experiments are summarized in Table 2.

EXPERIMENTAL RESULTS

Values of the solid/liquid distribution coefficients determined in this study are given in Table 2, along with some previously determined coefficients from Weill and McKay (1975). These distribution coefficients have been determined specifically for the range of composition and temperature appropriate to equilibria along the plagioclase-olivine cotectic and near the plagioclase-olivine-pyroxene peritectic in the system $(Mg,Fe)_2SiO_4$-$CaAl_2Si_2O_8$-SiO_2. Attempts to apply the coefficients to systems with substantially different phase chemistry involves an uncertain extrapolation which should be approached with caution. Only the plagioclase/liquid distribution coefficients for Eu and the orthopyroxene/liquid and olivine/liquid coefficients for Cr show significant dependence on oxygen fugacity. In Fig. 2 we have plotted $D^{Cr}_{px/liq}$ and $D^{Cr}_{ol/liq}$ as a function of oxygen fugacity. As in the case of Eu in plagioclase and Ca-pyroxene (Weill and Drake, 1973; Weill et al. 1974), these data can be most easily interpreted in terms of variations of the fractions of the cation, in this case Cr, in the divalent and trivalent states. These variations may be expressed as an overall Cr distribution coefficient, $D = D_2(Cr^{+2}) + D_3(Cr^{+3})$. According to this interpretation the data plotted in Fig. 2 indicate that $D_3 > D_2$ both for olivine and orthopyroxene. The difference is more pronounced in orthopyroxene. Schreiber and Haskin (1976) have published some experimental distribution coefficients for Cr in enstatite, diopside and forsterite. Their determinations were carried out using iron-free synthetic compositions including one (their composition FAS) lying within the ternary system Mg_2SiO_4-$CaAl_2Si_2O_8$-SiO_2. Composition FAS has some obvious similarities to the compositions used in this study (near the peritectic point in the pseudoternary system $(Mg,Fe)_2SiO_4$-$CaAl_2Si_2O_8$-SiO_2) although compositions in the iron-free system have higher liquidus temperatures than the corresponding Fe-bearing liquids lying at the same point in the pseudoternary diagram. Because of the differences between the compositions investigated by Schreiber and Haskin and those which we investigated, and because the lowest temperature for which they determined Cr distribution coefficients (1300°C) is considerably higher than the

temperature at which we determined coefficients (1200°C), their results cannot be directly compared with ours. Nevertheless, the results of the present study have several important general features in common with the results of Schreiber and Haskin for their composition FAS: both studies show D^{Cr} decreasing with decreasing f_{O_2} (at $f_{O_2} < 10^{-6}$) in both orthopyroxene and olivine, with the magnitude of the decrease being much larger for orthopyroxene; we infer from the variation of the D's with f_{O_2} that a substantial fraction of the Cr in our experimental liquids is divalent at 1200°C and f_{O_2} of 10^{-13} (we are unable to quantitatively determine the value of this fraction), while Schreiber and Haskin find that more than 75% of the Cr in their liquids (as measured by titration and EPR) is divalent at 1300°C and f_{O_2} of 10^{-10}; we find that for orthopyroxene $D_3 > 9$ at 1200°C, while Schreiber and Haskin find that $D_3 > 7$ at 1300°C. Values of $D^{Eu}_{pl/liq}$, $D^{Cr}_{px/liq}$ and $D^{Cr}_{ol/liq}$ appropriate to the lunar range of T-f_{O_2} are given in Table 2.

DISCUSSION

A highly evolved KREEP sample - 15386

In terms of major element composition, sample 15386 is the most evolved member of the KREEP suite shown in Fig. 1. Its bulk composition places it along the plagioclase-pyroxene saturation curve, down-temperature from the olivine-pyroxene-plagioclase peritectic point. It is one of the relatively few samples of KREEP with unmistakably igneous texture, and its low Ni content (Nyquist et al, 1975), implying a low amount of meteoritic contamination, further enhances the likelihood that its immediate origins were igneous. According to the phase equilibrium diagram of Fig. 1, a liquid of composition 15386 is an intermediate product of differentiation (via either partial melting or crystallization) of a parental composition near the peritectic point. The pseudoternary phase diagram and the distribution coefficient $D^{Fe/Mg}_{px/liq}$ may be combined with the known Mg and Fe contents of 15386 to determine the major element concentrations in a model parent P (Table 1 and Fig. 5) and the relative

proportions of coexisting plagioclase, pyroxene and liquid 15386. Fortunately 15386 is a very well documented Apollo 15 crystalline KREEP sample. In addition to its major element content, there are reliable trace element and whole rock Rb/Sr data, as well as an internal Rb/Sr isochron age. The known trace element concentrations in 15386 allow us to calculate the trace element concentrations in parental composition P according to the mass balance equation for each trace element:

$$\overline{D} = \sum_{i=1}^{n} D_i W_i = (C_o - C_L F)/(1 - F)C_L \qquad [1]$$

where $\overline{D}$ is the composite solid/liquid distribution coefficient, D_i is the distribution coefficient and W_i is the weight fraction of mineral i ($\sum_{i=1}^{n} W_i \equiv 1$), while F is the weight fraction of the equilibrated liquid relative to the total weight of the system. C_L is the concentration of the trace element in the liquid (i.e. 15386) and C_o is the concentration of the trace element in the total system (i.e., parental composition P). In Table 1 we have listed the major and trace element data for 15386 and its model parent composition P. Plagioclase is involved in the differentiation step P → 15386, and because $D^{Sr}_{pl/liq}$ is very nearly one hundred times greater than $D^{Rb}_{pl/liq}$, this step also involves an increase of Rb/Sr from 0.061 in composition P to 0.099 in 15386. We will return to this point in discussing the Rb/Sr isotopes.

Possible relationship between peritectic KREEP and other highland rocks

The peritectic point of the pseudoternary phase diagram is obviously an important composition. Many of the KREEP rocks plot close to this point, and we have also just discussed the possibility that such liquids are parental to some of the more evolved KREEP samples such as 15386. Mineral assemblages of olivine + plagioclase + pyroxene produce initial melts of the peritectic composition. Conversely, during crystallization in the "highlands" systems residual liquid compositions approach the peritectic. It is desirable therefore to consider the question

of the possible origin of KREEP peritectic liquids and examine whether there are any rock compositions in the highlands which could have given rise to KREEP-rich peritectic liquids via either equilibrium crystallization or partial melting. In pursuing this question we will use two typical examples of KREEP "peritectic" compositions; the possible parent of 15386 which we have just calculated (model composition P) and the soil 14163 which is representative of Apollo 14 KREEP breccias and plots very close to the peritectic in Fig. 1. Both of these compositions are given in Table 1. In keeping with our previous discussion we assume that the evolution to liquids P and 14163 was governed by liquid-solid differentiation and that the trace element partitioning is described by the mass balance of equation [1]. The refractory solid phase assemblages involved are combinations of plagioclase, pyroxene and olivine. The peritectic liquid is assumed to be essentially equilibrated with these mineral assemblages either after partial melting or crystallization of the parent material. As candidates for parental materials to peritectic liquids we have considered highland rocks (approximately 80) for which we could find published major and trace element analyses of the same subsample.

There are many sets and subsets of abundance criteria which could be used as filters to select the potential parents of KREEP-rich peritectic liquids. Our distribution coefficient data (Table 2) include typical "excluded" (i.e., trivalent) REE, an atypical REE (Eu) and the important major elements Mg and Fe. The approach we have employed is first to determine, for each of the parental candidates, the relative proportions of each phase which must be present in the equilibrated assemblage (i.e., peritectic liquid plus solids) in order that the liquid have the same content of the excluded trace element Sm as that observed in 14163 or composition P. We then check whether these relative

phase proportions would also yield a liquid with the abundances of Eu and Mg/(Mg + Fe) observed in 14163 or composition P. The calculations proceed as follows: (1) We first assign a value of $\overline{D} = 0$ for Sm. This allows an approximate calculation of F according to equation 1. At this point we arbitrarily reject candidates for which $F > 0.8$ since such materials are already so enriched in KREEP components that they are of little interest in considering the parentage of KREEP. For the remaining candidates, we use the approximate value of F to calculate the approximate bulk composition (and hence the mode) of the residual solid assemblage according to the simple mass balance relationship, $C_o = FC_L + (1 - F)C_S$, where C_o is the observed concentration of a major element in the potential parent, C_L is the concentration in 14163 or P, and C_S is the concentration in the residual solid assemblage. The approximate mode in turn allows a refined value of $\overline{D}_{Sm}$ to be calculated (equation 1) using the individual mineral distribution coefficients for Sm from Table 2. The refined $\overline{D}_{Sm}$ is in turn used to calculate a refined value for F, etc., etc. The iterations are terminated when successive solutions of F differ by less than 10% relative. (2) The final value for F and the corresponding mode of the refractory solid assemblage are then combined with the distribution coefficients for Eu, Mg and Fe (Table 2) in equation [1] to calculate the Eu and Mg/(Mg + Fe) abundances in the liquid.

The calculated abundances of Eu and Mg/(Mg + Fe) for each candidate parent are plotted in Fig. 3 where they are compared to 14163. The rectangle around 14163 represents estimates of the combined uncertainties in the distribution coefficients of Sm, Eu, Fe and Mg. Highland rocks which are potential parental compositions for 14163 must plot within the rectangle of Fig. 3. Note that the average highland composition of Taylor and Jakeš (1974) produces a liquid with the appropriate Sm and Eu content but too little Mg/(Mg + Fe) as pointed out by Weill and McKay (1975). We next consider whether there is anything distinctive about the bulk compositions

of samples which qualify as potential parents to 14163. In Fig. 4a we have plotted all candidates tested. The compositions span nearly the entire range of highland rock types. In Fig 4b we have plotted all candidates that meet the criteria for parental material. The large majority of them are close to the olivine-plagioclase cotectic. A similar set of calculations was repeated using composition P as the daughter liquid instead of 14163, and the results were very similar. Since the criteria were completely independent of the location of the phase saturation boundaries, the results may be interpreted as independently reinforcing the notion that many of the KREEP suite of rocks are related by the phase equilibria depicted in Fig. 1.

In all, 33 highland rock compositions were found to be potential parents for peritectic liquids P or 14163. The average composition of all these potential parents is given as composition C in Table 1. This average is very similar to the Apollo 15 Low-K Fra Mauro (LKFM) basalt type (also shown in Table 1) proposed by Reid et al.(1972). Taylor and Jakeš (1974) concluded on the basis of orbiter data that the LKFM composition is an abundant constituent of the lunar highlands. Thus, the constraints of low pressure phase equilibria and of major and trace element partitioning are satisfied by models which relate KREEP peritectic liquids (and their possible derivatives such as 15386) to an abundant crustal rock type via equilibrium crystallization and partial melting.

Possible origin of KREEP

We have shown that it is possible to consider the KREEP-rich rocks as an igneous suite evolved by solid-liquid differentiation along the crystal saturation boundaries of the highlands pseudoternary phase equilibrium diagram. The least evolved members of this suite plot along the olivine-plagioclase cotectic with an average composition corresponding to point C in Fig. 5. The ultimate origin of such liquids is a question which may never be answered and certainly will be extremely

difficult to answer in any detail. Nevertheless it is tempting to consider that a liquid which plots near the olivine–plagioclase boundary originated by equilibrium processes governed by the phase relations of Fig. 1, i.e., by partial melting or crystallization, at pressures somewhat less than 10 kilobars, of a bulk system which lies ~~with~~ within the $(Mg,Fe)_2SiO_4$-SiO_2-$CaAl_2Si_2O_8$ system. If this model is assumed to be strictly valid then it is possible to "solve" the problem with an approach described by Weill and McKay (1975). Using distribution coefficients for Sr and the REE measured for plagioclase and olivine and assuming some initial value for the concentration of these elements in the parental material, the mass balance equations [1] for these trace elements can be solved for the fraction of liquid C and the proportions of plagioclase and olivine in the equilibrated solid assemblage. This solid assemblage, when added to the liquid C, constitutes the parental material. In the present calculations we have assumed an initial concentration of 5X chondritic levels for the LIL in the parental material. Crystallization experiments in the pseudoternary system (Weill and McKay, 1975) indicate that liquid C is equilibrated with plagioclase and olivine at approximately 1250°C, and we interpolated the plagioclase distribution coefficients of Table 2 to this temperature. The temperature dependence of olivine distribution coefficients is not known and we have adopted the values at 1200°C. $D^{Sr}_{ol/liq}$ was assumed to be similar to $D^{Eu}_{ol/liq}$ under strongly reducing conditions.

The best fit (using least squares criteria applied to solutions of equation [1] for each of the trace elements) to these data yields a parental composition shown as C' in Fig. 5. If this material originally had 5x chondritic abundances of LIL, then approximately 4 wt % of liquid equilibrated with a solid assemblage dominated by olivine and plagioclase would have an LIL abundance pattern closely approximating that of KREEP-rich composition C. There are many factors which prevent a rigorous assessment of such results. Among others, we can list the more obvious ones:

(1) Modest departures of bulk composition as well as increased pressure can result in

appreciably different "phase diagrams" such that liquid C is not necessarily saturated with olivine and plagioclase as we have assumed. (2) The assumption that the LIL elements in the parental material have a primitive lunar (i.e., flat 5X chondritic) abundance pattern is somewhat arbitrary. (3) If the source of KREEP was itself formed as a direct or indirect consequence of fractionation in a ' lunar magma ocean, then there is always the possibility that the source mineralogy and bulk composition was dominated by cumulates while the trace element abundances were influenced by varying amounts of intercumulus liquid. In view of these and other uncertainties we believe that these calculations simply show that if the KREEP-rich liquid precursors (e.g., liquid C) to the highly evolved igneous KREEP samples (e.g., 14163 and 15386) were derived from primitive lunar systems under conditions approaching equilibrium partitioning of trace elements, then that source material must have been rich in olivine and contained much smaller amounts of plagioclase. This is essentially the same general theme that emerged from our previous modeling (Weill and McKay, 1975) which considered the generation of evolved KREEP (for instance, near-peritectic liquids) by one-step partial melting of assemblages resembling the whole moon in bulk composition.

Rb-Sr isotopes

The plagioclase/liquid distribution coefficients for Sr and Rb differ by almost two orders of magnitude (Table 2). Any fractionation step in the evolution of the KREEP suite which involves plagioclase and liquid will therefore result in a change of Rb/Sr. We now consider whether the models we have proposed are consistent with the Rb/Sr isotopic data. If a closed system inherited a radiogenic strontium content denoted by $(^{87}Sr/^{86}Sr)_o$ at some time, T_o, before the present, then the present $(^{87}Sr/^{86}Sr)_p$ and $(^{87}Rb/^{86}Sr)_p$ are given by:

$$(^{87}Sr/^{86}Sr)_p - (^{87}Sr/^{86}Sr)_o = (^{87}Rb/^{86}Sr)_p \, (e^{\lambda T_o} - 1) \qquad [2]$$

where $\lambda = 1.39 \times 10^{-11}$ yr^{-1} is the ^{87}Rb decay constant. Only if a system has actually remained closed to Rb/Sr fractionation between T_o and the present does T_o really correspond to a time in the past when the system inherited $(^{87}Sr/^{86}Sr)_o$. However, according to equation [2], if a system is assigned a value of $(^{87}Sr/^{86}Sr)_o$, a value of T_o can always be calculated regardless of whether the system has actually undergone Rb/Sr fractionation or not. For a system which has suffered Rb/Sr fractionation, T_o has no real significance except to denote the time in the past when

the system would have inherited $(^{87}Sr/^{86}Sr)_o$ had it evolved without Rb/Sr fractionation. For this reason, T_o is usually referred to as a model "age" and given the notation T_M or T_{IR} where the subscripts signify model and assigned initial ratio of $(^{87}Sr/^{86}Sr)$ respectively.

Schoenfeld and Meyer (1972) have shown that if a system actually inherited $(^{87}Sr/^{86}Sr)_o$ at T_o and subsequently underwent a Rb/Sr fractionation step at T_1, then the model age defined by equation [2] is given by

$$e^{\lambda T_M} = e^{\lambda T_1} + \frac{(e^{\lambda T_o} - e^{\lambda T_1})}{R_1} \qquad [3]$$

where $R_1 = \dfrac{(Rb/Sr)_{differentiate}}{(Rb/Sr)_{parent}}$

Schoenfeld (1976) extended the same approach to consider two fractionation steps, and it can easily be shown that for three fractionation steps

$$e^{\lambda T_M} = \frac{(e^{\lambda T_o} - e^{\lambda T_1})}{R_1R_2R_3} + \frac{(e^{\lambda T_1} - e^{\lambda T_2})}{R_2R_3} + \frac{(e^{\lambda T_2} - e^{\lambda T_3})}{R_3} + e^{\lambda T_3} \qquad [4]$$

We now apply the formalism outlined above to the models we have discussed for the evolution of the various members of the KREEP suite. In the calculations we have adopted values of T_o = 4.60 b.y. and $(^{87}Sr/^{86}Sr)_o$ = 0.69903 (LUNI of Nyquist et al., 1974). Most of the whole-rock isotopic data we use were determined by Nyquist and coworkers. We have also used data determined by Papanastassiou and coworkers and have adjusted $(^{87}Sr/^{86}Sr)$ for interlaboratory bias. None of our arguments are significantly affected by changes of ±0.5 b.y. in T_o or by adopting $(^{87}Sr/^{86}Sr)_o$ = 0.69898 (BABI of Papanastassiou et al., 1969).

Composition C (Fig. 5) is the least evolved of the KREEP suite we have discussed and may be a precursor type for the other members of the suite. In Table 1 we have listed averages of published Rb/Sr isotopic data for rocks that met the criteria for parental material of 14163 or the calculated P composition. The details of petrogenesis for liquids with compositions close to C are not known, but for the present discussion we need simply to adopt the view that compositions of this type were produced in a single differentiation step from primitive lunar materials. Equation [3] may be solved for T_1 vs. R_1. The solution is shown in Fig. 6. If we adopt the value of $(Rb/Sr)_{parent}$ = 0.0067 as proposed for the whole moon by Taylor and Jakeš (1974), the time of the differentiation step is 4.44 b.y. This value is essentially equal to the 4.42 b.y. proposed by Tera and Wasserburg (1974) on the basis of U-Pb isotopes for the time of large scale differentiation of the moon.

We have seen that liquids of cotectic composition C may be typical of the KREEP-rich precursors of more highly evolved KREEP samples such as 15386. According to our model, 15386 may be the result of three differentiation steps;
primitive parent $\xrightarrow{T_1}$ C $\xrightarrow{T_2}$ P $\xrightarrow{T_3}$ 15386. The internal isochron age of 15386 is 3.94 b.y. (Nyquist et al., 1975) and the simplest interpretation is to equate this with T_3, the time of the most recent differentiation. $(^{87}Rb/^{86}Sr)$

values for the whole moon, compositions C and P and 15386 are all listed in Table 1, and these values fix R_1, R_2, and R_3. Furthermore, T_1 = 4.44 b.y. and T_3 = 3.94 b.y., and we can solve equation [4] for the model age of 15386 vs. T_2. The solution is shown in Fig. 7. The model age of 15386 (T_{LUNI}) is 4.26 b.y., corresponding to T_2 = 4.41 b.y. This result is not at all sensitive to variations in $(^{87}Sr/^{86}Sr)_o$. It is somewhat sensitive to variations in the last fractionation step, but it is not possible to place meaningful accuracy limits on R_3. However, R_3 is calculated from data which ~~is~~ are independent of the isotopic data, and we believe that the result $T_2 \simeq T_1$ is not fortuitous. The production of liquid C and the subsequent differentiation to liquid P in a short time is appealing from a physical point of view. It is difficult to store a liquid for long periods ~~on~~ in the moon, and the alternative would require a later heat source to remelt C.

The present-day isotopic ratios of P, C and 15386 are shown in Fig. 8 along with those of Apollo 14 and 15 crystalline KREEP samples and some of the KREEP-rich ~~KREEPy~~ rocks found to be possible parents for 14163 and composition P. Also shown is the isotopic composition of the whole moon (M) calculated from the whole moon Rb/Sr of Taylor and Jakeš (1974), the $(^{87}Sr/^{86}Sr)_o$ = LUNI of Nyquist et al. (1974) and T_o = 4.60 b.y. M, C, and P, as well as the possible parents of P, lie very close to the 4.44 b.y. isochron, while the Apollo 14 and 15 crystalline KREEP rocks are part of the 3.94 b.y. isochron defined by P and 15386.

Another perspective of the Rb/Sr isotope evolution of these samples is shown in Fig. 9A where we plot the isotopic compositions of the samples 3.94 b.y. ago calculated on our model assumption that no Rb/Sr fractionation has occurred since that time. Most of the Apollo 14 and 15 crystalline KREEP samples have the same $(^{87}Sr/^{86}Sr)$ as P and 15386 within analytical error limits, consistent with the production of these evolved KREEP samples 3.94 b.y. ago by an igneous process which involved variable enrichments of $(^{87}Rb/^{86}Sr)$. The logical candidate for such

a process is partial melting of crystallized P or fractional crystallization of liquid P. The ~~KREEPy~~ KREEP-rich samples that were found to have compositions that could be parental to peritectic liquids are still on the isochron defined by M, C and P, indicating that these samples were not appreciably fractionated 3.94 b.y. ago.

In Fig. 9B we have plotted the isotopic compositions as they would have been 4.44 b.y ago. The crystalline Apollo 14 and 15 KREEP samples are not included because they did not exist as such according to our working model. The ~~KREEPy~~ KREEP-rich precursors to KREEP peritectic liquids all have ($^{87}Sr/^{86}Sr$) identical to the whole moon and P. The spread of ($^{87}Rb/^{86}Sr$) at this time is consistent with derivation of a suite of liquids from a primitive lunar composition. Note that it would be possible to generate a range of Rb/Sr values in such liquids by varying the relative proportions of liquid to crystalline material (most importantly, plagioclase). Composition P is just one possible member of the suite generated at this time. In general, compositions close to P would be equilibrated with more residual plagioclase (and hence undergo greater increases of ($^{87}Rb/^{86}Sr$) relative to M) than liquids further up temperature on the olivine-plagioclase cotectic. Also, since it is possible for a liquid of peritectic composition to coexist with variable amounts of plagioclase we could even expect that peritectic liquids (as defined by their major element composition) derived at this time might have variable ($^{87}Rb/^{86}Sr$). The composition P shown in our plot is just one of the series singled out because of its calculated parental relationship to 15386. If another member of the series generated 4.44 b.y. ago subsequently differentiated at 3.94 b.y., its daughters would have inherited somewhat higher or lower ($^{87}Sr/^{86}Sr$) at that time (cf. the Apollo 14 and 15 crystalline KREEP in Fig. 9A).

SUMMARY

The model which we have presented to account for a range of ~~KREEPy~~ KREEP-rich lunar rocks is summarized in Fig. 10. It relates much of the KREEP suite in a scheme of igneous differentiation which is consistent with major and trace element concentrations, the general features of experimentally determined phase equilibria and Rb-Sr evolution. The "proto-KREEP" from which more evolved KREEP is derived strongly resembles a common highland rock type, the low-K Fra Mauro basalts. Although the model describes a possible three-step evolution for the more evolved crystalline KREEP samples such as 15386, the most probable time scale according to the isotopic data only allows resolution of two igneous activity pulses. The formation of the highly evolved 15386 occurred during igneous activity about 3.9 b.y. ago, at a time when the rate of impacts on the lunar surface had slowed down and mare basalt generation was beginning.

The origin of the KREEP precursors (LKFM(?) ⟶ peritectic liquid types) at 4.4 b.y. is not well delineated but most probably involved liquid differentiation from a relatively primitive lunar source which contained much olivine and less plagioclase. We cannot rule out the possibility that a limited amount of other refractory mineral phases was also left behind after this liquid type was generated. Many of the KREEP-rich systems derived at this time do not seem to have been subsequently strongly disturbed in major, trace or isotopic composition.

Acknowledgments

Our research is supported by NASA grants NGL 38-003-020 and NGL 38-003-022.

REFERENCES

Baedecker P., Chou C.-L, Grudewicz E. and Wasson, J. (1973) Volatile and siderophille trace elements in Apollo 15 samples: Geochemical implications and characterization of the long-lived and short-lived extralunar materials. *Proc. Lunar Sci. Conf. 4th*, p. 1177-1195.

Drake M., Stoeser J. and Goles G. (1973) A unified approach to a fragmental problem: petrological and geochemical studies of lithic fragments from Apollo 15 soils. *Earth Planet. Sci. Lett. 20*, p. 425-439.

Ganapathy R. and Anders E. (1974) Bulk compositions of the moon and earth estimated from meteorites. *Proc. Lunar Sci. Conf. 5th*, p. 1181-1206.

Haskin L., Helmke P., Blanchard D., Jacobs J. and Telander K. (1973) Major and trace element abundances in samples from the lunar highlands. *Proc. Lunar Sci. Conf. 4th*, p. 1275-1296.

Hubbard N., Gast P., Rhodes J., Bansal B. and Wiesmann H. (1972) Nonmare basalts: Part II. *Proc. Lunar Sci. Conf. 3rd*, p. 1161-1179.

Hubbard N., Rhodes J., Gast P., Bansal B., Shih C., Wiesmann H. and Nyquist L. (1973) Lunar rock types: The role of plagioclase in nonmare highland rock types. *Proc. Lunar Sci. Conf. 4th*, p. 1297-1312.

Laul J., Wakita H., Showalter D., Boynton W. and Schmitt R. (1972) Bulk, rare earth, and other trace elements in Apollo 14 and 15 and Luna 16 samples. *Proc. Lunar Sci. Conf. 3rd*, p. 1181-1200.

LSPET (1972) The Apollo 15 lunar samples: a preliminary description. *Science 175*, p. 363-375.

LSPET (1973) The Apollo 16 lunar samples: Petrographic and chemical description. *Science 179*, p.23-24.

LSPET (1974) Apollo 17 lunar samples: Chemical and petrographic description. *Science 182*, p. 659-690.

Lugmair G., Kurtz J., Marti K. and Scheinin N. (1976) The low-Sm/Nd region of the moon: Evolution and history of a troctolite and a KREEP basalt (abstract). In *Lunar Science VII*, p. 509-511. The Lunar Science Institute, Houston.

Nava D. (1974) Chemical compositions of some soils and rock types from the Apollo 15, 16 and 17 lunar sites. *Proc. Lunar Sci. Conf. 5th*, p. 1087-1096.

Nakamura N., Masuda A., Tanaka T. and Kurasawa H. (1973) Chemical compositions and rare-earth features of four Apollo 16 samples. *Proc. Lunar Sci. Conf. 4th*, p. 1407-1414.

Nyquist L., Hubbard N., Gast P., Bansal B. and Wiesmann H. (1973) Rb-Sr systematics for chemically defined Apollo 15 and 16 materials. *Proc. Lunar Sci. Conf. 4th*, p. 1823-1846.

Nyquist L., Bansal B., Wiesmann H. and Jahn B.-M. (1974) Taurus-Littrow chronology: Some constraints on early lunar crustal development. *Proc. Lunar Sci. Conf. 5th*, p. 1515-1539.

Nyquist L., Bansal B. and Wiesmann H. (1975) Rb-Sr ages and initial $^{87}Sr/^{86}Sr$ for Apollo 17 basalts and KREEP basalt 15386. *Proc. Lunar Sci. Conf. 6th*, p. 1445-1465.

Papanastassiou D. and Wasserburg G. (1971) Rb-Sr ages of igneous rocks from the Apollo 14 mission and the age of the Fra Mauro Formation. *Earth Planet. Sci. Lett. 12*, p. 36-48.

Philpotts J., Schnetzler C., Nava P., Bottino M., Fullager P., Thomas H., Schuhmann S. and Kouns C. (1972) Apollo 14: Some geochemical aspects. *Proc. Lunar Sci. Conf. 3rd*, p. 1293-1305.

Philpotts J., Schuhmann S., Kouns E., Lum R. and Winzer S. (1974) Origin of Apollo 17 rocks and soils. *Proc. Lunar Sci. Conf. 5th*, p. 1255-1267.

Rhodes J. and Hubbard N. (1973) Chemistry, classification, and petrogenesis of Apollo 15 mare basalts. *Proc. Lunar Sci. Conf. 4th*, p. 1127-1148.

Rhodes J., Rodgers K., Shih C., Bansal B., Nyquist L., Wiesmann H. and Hubbard N. (1974) The relationships between geology and soil chemistry at the Apollo 17 landing site. *Proc. Lunar Sci. Conf. 5th*, p. 1097-1117.

Ried A., Warner J., Ridley W. and Brown R. (1972) Major element compositions of glasses in the three Apollo 15 soils. *Meteorites 7*, p. 395-415.

Rose H., Cuttita F., Annell C., Curron M., Christian R., Dwornik E., Greenland L. and Ligon D. (1972) Compositional data for twenty-one Fra Mauro lunar materials. *Proc. Lunar Sci. Conf. 3rd*, p. 1215-1279.

Schoenfeld E. and Meyer C. (1972) The abundances of components of the lunar soils by a least-squares mixing model and the formation age of KREEP. *Proc. Lunar Sci. Conf. 3rd*, p. 1397-1420.

Schoenfeld E. (1976) Rb-Sr evolution of the lunar crust (abstract). In *Lunar Science VII*, p. 773-775. The Lunar Science Institute, Houston.

Schreiber H. and Haskin L. (1976) Cr(III)-Cr(II) distribution coefficients in synthetic silicate systems in relation to the partition of

chromium on the Moon (abstract). In *Lunar Science VII*, 776-778. The Lunar Science Institute, Houston.

Taylor S. (1973) Geochemistry of the lunar highlands. *The Moon 7*, p. 181-195.

Taylor S., Gorton M., Muir P., Nance W., Rudowski R. and Ware N. (1973) Lunar highlands composition: Apennine Front. *Proc. Lunar Sci. Conf. 4th*, p. 1445-1459.

Taylor S. and Jakeš P. (1974) The geochemical evolution of the moon. *Proc. Lunar Sci. Conf. 5th*, p. 1287-1305.

Taylor S., Kaye M., Muir P., Nance W., Rudowski R. and Ware N. (1972) Composition of the lunar uplands: Chemistry of Apollo 14 samples from Fra Mauro. *Proc. Lunar Sci. Conf. 3rd*, p. 1231-1249.

Terra F. and Wasserburg G. (1974) U-Th-Pb systematics in lunar rocks and inferences about lunar evolution and the age of the moon. *Proc. Lunar Sci. Conf. 5th*, p. 1571-1599.

Walker D., Longhi J., Grove T., Stolper E. and Hays J. (1973) Experimental petrology and origin of rocks from the Descartes Highlands. *Proc. Lunar Sci. Conf. 4th*, p. 1013-1032.

Walker D., Longhi J. and Hays J. (1972) Experimental petrology and the origin of Fra Mauro rocks and soil. *Proc. Lunar Sci. Conf. 3rd*, p. 797-817.

Wänke H., Baddenhausen H., Balacescu A., Teschke F., Spettel B., Dreibus G., Palme H., Quijano-Rico M., Kruse H., Wlotzka F. and Begemann F. (1972) Multielement analyses of lunar samples and some implications of the results. *Proc. Lunar Sci. Conf. 3rd*, p. 1251-1268.

Wasserburg G. and Papanastassiou D. (1971) Age of an Apollo 15 mare

basalt: Lunar crust and mantle evolution. *Earth Planet. Sci. Lett. 13*, p. 97-104.

Weill D. and Drake M. (1973) Europium anomaly in plagioclase feldspar: Experimental results and semiquantitative model. *Science 180*, p. 1059-1060.

Weill D. and McKay G. (1975) The partitioning of Mg, Fe, Sr, Ce, Sm, Eu and Yb in lunar igneous systems and a possible origin of KREEP by equilibrium partial melting. *Proc. Lunar Sci. Conf. 6th*, p. 1143-1158.

Weill D., McKay G., Kridelbaugh S., and Grutzeck M. (1974) Modeling the evolution of Sm and Eu abundances during lunar igneous differentiation. *Proc. Lunar Sci. Conf. 5th*, p. 1337-1352.

Wiesmann H. and Hubbard N. (1975) A compilation of the lunar sample data generated by the Gast, Nyquist and Hubbard lunar sample PI-ships. NASA Johnson Space Center. Unpublished manuscript.

Table 1. Major element, trace element and Rb-Sr isotopic compositions of several members of the KREEP suite. The average highlands and whole Moon compositions proposed by Taylor and Jakeš(1974) are given for comparison. See Figures 3 and 8 for sources of data.

	15386	14163	P[1]	C[2]	LKFM[3]	HL[4]	WM[5]
wt%							
SiO_2	50.8	48.0	49.1	45.8	46.6	44.9	44.0
TiO_2	2.2	1.8	2.3	1.3	1.3	0.6	0.3
Al_2O_3	14.8	17.6	15.9	19.0	18.8	24.6	8.2
FeO	10.6	10.4	8.2	8.6	9.7	6.6	10.5
MgO	8.2	9.2	11.8	12.7	11.0	8.6	31.0
CaO	9.7	11.2	12.1	11.3	11.6	14.2	6.0
ppm							
Rb	18.5	13	11	5.6	2.7	1.7	0.3
Sr	187	180	180	167	140	200	43
Ce	211	200	126	78	81	22.	3.1
Sm	37	32	22	14	13	3.3	0.8
Eu	2.7	2.8	2.2	1.8	1.8	1.7	0.3
Yb	24	24	15	9.7	9.8	2.3	0.7
$^{87}Sr/^{86}Sr$	0.71640		0.71049	0.70619[7]			
$^{87}Rb/^{86}Sr$	0.285		0.180	0.112			
T_{LUNI}[6](AE)	4.26		4.45	4.47			

1. Peritectic liquid which may have been parental to 15386. Composition calculated from 15386 as explained in text.

Table 1. (continued)

2. Average of samples found to be potential parents to P and/or 14163.

3. Apollo 15 Low-K Fra Mauro basalt of Reid et al.(1972). Trace element composition from Taylor(1973).

4. Proposed average composition of highland crust (Taylor and Jakeš, 1974).

5. Proposed composition of whole moon (Taylor and Jakeš, 1974).

6. $^{87}Sr/^{86}Sr_{LUNI}$ = 0.69903 (Nyquist et al., 1974).

Table 2. Experimentally determined crystal/liquid distribution coefficients (wt. basis) for ilmenite, plagioclase, Ca-poor pyroxene and olivine. Values in italics are from Weill and McKay(1975). Other values are from the present study. The uncertainty generally represents the standard deviation of the mean of a number of determinations. Representative compositions of coexisting phases are given in notes a-f.

	Ilm[a] (1140°C)	Plag[b] (1340°C)	Plag[c] (1200°C)	Px[d] (1340°C)	Px[e] (1200°C)	Ol[f] (1200°C)
Sr		*1.53 ±.02*	*1.63 ±.06*	*.009 ±.006*	*.018 ±.003*	
Ce	.006 ±.003	*.062 ±.002*	*.048 ±.001*	*.006 ±.002*	*.009 ±.002*	.010 ±.007
Sm	.010 ±.002	*.044 ±.002*	*.032 ±.002*	*.013 ±.005*	*.022 ±.001*	.015 ±.005
Eu	.007 ±.003	*1.1*[g]	*1.0*[g]	*.014 ±.003*	*.022 ±.002*	.015 ±.005
Yb	.075 ±.005	*.031 ±.002*	*.028 ±.003*	*.056 ±.010*	*.170 ±.010*	.033 ±.002
Rb			.017 ±.008			
Ba			.15 ±.03		.011 ±.005	
Cr					5.2[g]	1.2[g]
Fe				*.54*	*.83*	*1.32*
Mg				*2.26*	*3.19*	*4.78*

Oxide values are in weight %. To facilitate location in the pseudoternary diagram (Fig. 1), mole % silica (SI), anorthite (AN), and olivine (OL) are given for glasses other than mare basalt.

a. Ilmenite: TiO_2=55.9, Al_2O_3=0.37, FeO=34.5, MgO=7.07, Cr_2O_3=1.79

Glass: SiO_2=42.4, TiO_2=10.2, Al_2O_3=7.99, FeO=19.0, MgO=6.26, CaO=8.98, Cr_2O_3= 0.10

Table 2. (continued)

b. Plagioclase: SiO_2=44.7, Al_2O_3=36.2, FeO=0.29, MgO=0.42, CaO=19.8

Glass: SiO_2=48.0, TiO_2=.62, Al_2O_3=23.1, FeO=3.50, MgO=10.1, CaO=11.6 ($SI_{36}AN_{38}OL_{26}$)

c. Plagioclase: SiO_2=45.3, Al_2O_3=34.0, FeO=0.33, MgO=0.44, CaO=18.7

Glass: SiO_2=50.2, TiO_2=1.49, Al_2O_3=17.7, FeO=8.65, MgO=9.12, CaO=9.27 ($SI_{48}AN_{26}OL_{26}$)

d. Pyroxene: SiO_2=59.3, TiO_2=0.05, Al_2O_3= 0.53, FeO=4.34, MgO=36.9,CaO=0.26

Glass: SiO_2=57.4, TiO_2=.60, Al_2O_3=10.64, FeO=6.92, MgO=15.7, CaO=5.67 ($SI_{59}AN_{12}OL_{29}$)

e. Pyroxene: SiO_2=54.2, TiO_2= 0.3, Al_2O_3=5.3, FeO=8.7, MgO=30.4, CaO=1.3

Glass: SiO_2=48.9, TiO_2=1.10, Al_2O_3=16.6, FeO=9.37, MgO=8.90, CaO=9.23 ($SI_{48}AN_{25}OL_{27}$)

f. Olivine: SiO_2=40.3, FeO=13.6, MgO=46.2, CaO=0.20

Glass: SiO_2=48.6, TiO_2=.93, Al_2O_3=16.7, FeO=9.20, MgO=9.75, CaO= 9.04 ($SI_{46}AN_{25}OL_{29}$)

g. Values for $f_{O_2} = 10^{-13.0}$ at 1200°C and $10^{-11.4}$ at 1340°C. See Fig. 2 of this work and Fig. 5 of Weill and McKay (1975) for oxygen fugacity dependence. All other distribution coefficients are independent of f_{O_2} over the range of fugacities studied, $\log f_{O_2} = (6.57-27215/T) \pm 2$.

FIGURE CAPTIONS

Figure 1. Representation of bulk compositions of ~~KREEPy~~ KREEP-rich materials from Apollo 14-17 within $(Fe,Mg)_2SiO_4$-SiO_2-$CaAl_2Si_2O_8$ pseudoternary liquidus diagram. Average lunar highlands composition of Taylor and Jakeš(1974) is shown for comparison.

Figure 2. Variation of Cr distribution coefficients (weight basis) for olivine/liquid and orthopyroxene/liquid with oxygen fugacity. Error bars represent twice the standard deviation of the mean of a number of replicate determinations at each oxygen fugacity.

Figure 3. Calculated Eu contents and Mg/(Mg+Fe) of hypothetical peritectic liquids having the same Sm content as 14163. Each point represents the liquid produced by differentiation of a different highland sample. See text for details of the calculation. Actual Eu content and Mg/(Mg+Fe) of 14163 are indicated. Estimated uncertainties (±30% for Eu, ±20% for Mg/(Mg+Fe)) in calculated values for hypothetical liquids are indicated by the rectangle around 14163. Highland samples which are ~~possible~~ potential parents to 14163 must produce liquids which plot within this rectangle. Liquid produced from the average highlands composition of Taylor and Jakeš(1974) is indicated. Sources for data: Drake et al.(1973), Haskin et al.(1973), Hubbard et al.(1972,1973), Laul et al.(1972), LSPET(1972, 1973),Nava(1975), Nakamura et al.(1973), Philpotts et al.(1972,1974), Rhodes and Hubbard(1973), Rhodes et al.(1974), Rose et al.(1972), Taylor et al.(1972,1973), Wänke et al.(1972), and Wieśmann and Hubbard (1975).

Figure 4. (a) Pseudoternary projection of bulk compositions of highland samples tested ~~for possible paternity~~ as potential parents to 14163 ~~in Figure 3~~. (b) Bulk compositions of samples found to be ~~possible~~ potential parents to 14163, ie., samples generating liquids which plot within the rectangle surrounding 14163 in Figure 3.

Figure 5. Pseudoternary representations of important compositions in our model for the evolution of KREEP. P is the peritectic composition which differentiated to form 15386. 14163 is another example of a KREEP-rich peritectic ~~liquid~~ composition. C is the average composition of all highlands samples which are ~~possible~~ potential parents to P or 14163. C' is the composition of ~~the~~ a possible parent material to C, ~~assuming that the low pressure phase equilibria apply and that the parent to C had 5x chondritic LIL abundances~~ calculated as explained in the text. WM is the whole moon composition proposed by Taylor and Jakeš(1974).

Figure 6. Solution of Equation [3] for T_1, the time of formation of composition C (assuming a one-step process), vs. the amount of Rb/Sr fractionation occurring during its formation. The dotted vertical line is the Rb/Sr fractionation if C was formed from material with Rb/Sr as proposed by Taylor and Jakeš(1974) for the bulk moon. The dotted horizontal line is the resulting value of T_1.

Figure 7. Solution of Equation [4] for T_2, the time of ~~formation~~ differentiation of composition P from C, vs. the model age of 15386. If the bulk moon Rb/Sr of Taylor and Jakeš(1974) is adopted, R_1, R_2, and R_3 are fixed by the data in Table 1. T_1 is determined ~~by~~ in Figure 6, and T_3 is assumed to be 3.94 AE, the internal isochron age of 15386 (Nyquist et al., 1975). The dotted vertical line indicates the model age of 15386 reported by Nyquist et al.(1974), and the dotted horizontal line represents the resulting value of T_2. T_1 is indicated for comparison.

Figure 8. Rb-Sr evolution diagram showing presently observed or calculated isotopic ratios for 15386, P, C, and the whole moon (M). According to our model, M, C, and P define a 4.44AE isochron, while P and 15386 define a 3.94AE isochron. Isotopic ratios are also shown for a number of highland

samples which are ~~possible~~ potential parents to P (small p's) and a number of Apollo 14 and 15 crystalline KREEP samples (x's). Sources of data: Nyquist et al.(1973,1974,1975), Papanastassiou and Wasserburg(1971), and Wasserburg and Papanastassiou(1971).

Figure 9. Rb-Sr evolution diagrams showing isotopic ratios at time T, assuming closed system evolution from T until the present. Symbols are the same as in Figure 9. (a) T=3.94AE, the ~~time we prefer for the formation~~ time of crystallization of 15386 ~~from P~~. (b) T=4.44AE, the time we calculate for the formation of C and P from M.

Figure 10. Schematic representation of the model we propose for the origin of KREEP and the relationship between different ~~KREEPy~~ KREEP-rich materials. F is the fraction of liquid resulting from any differentiation step relative to the immediate parent material for that step.

FIG. 1

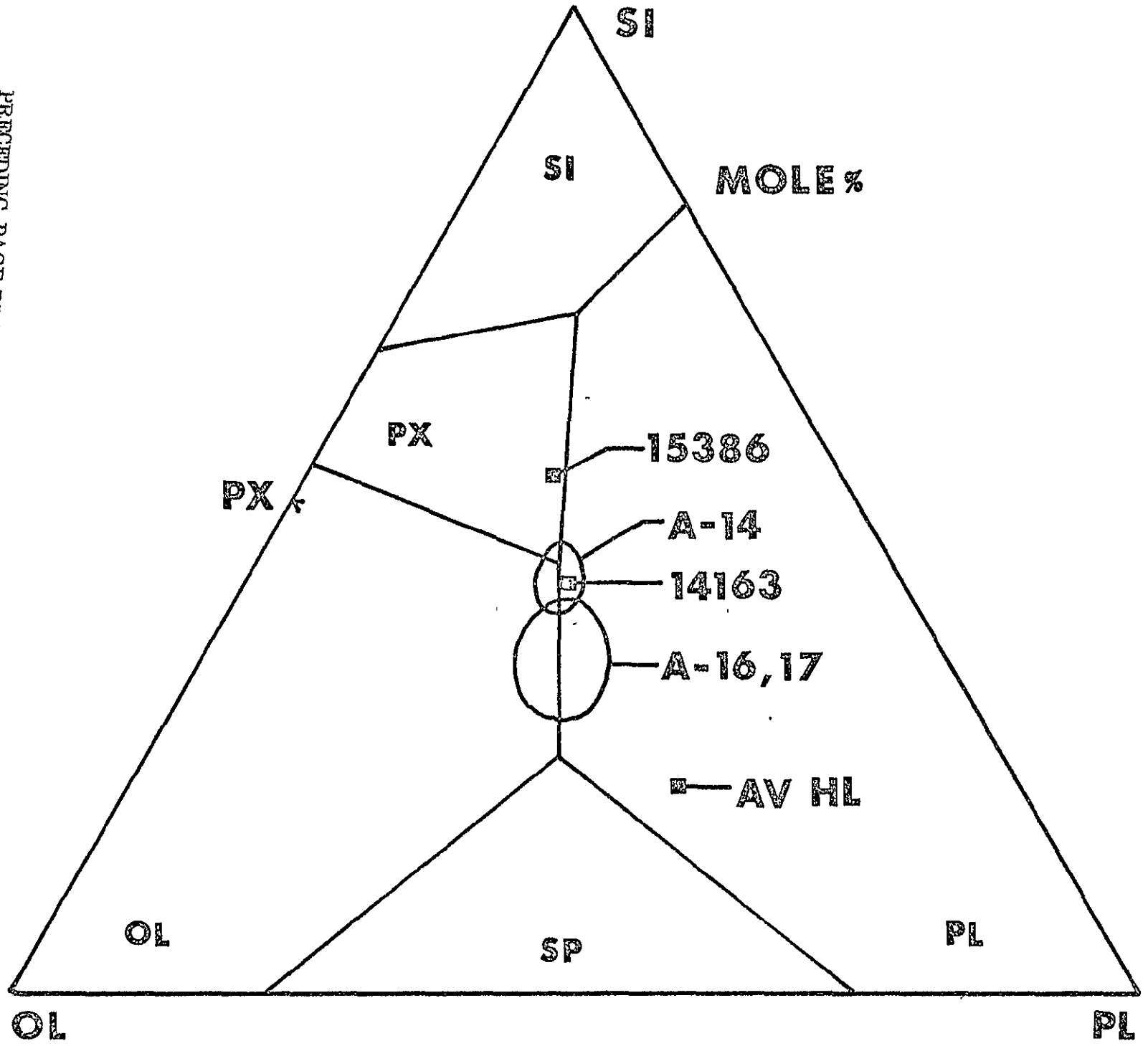

FIG. 2

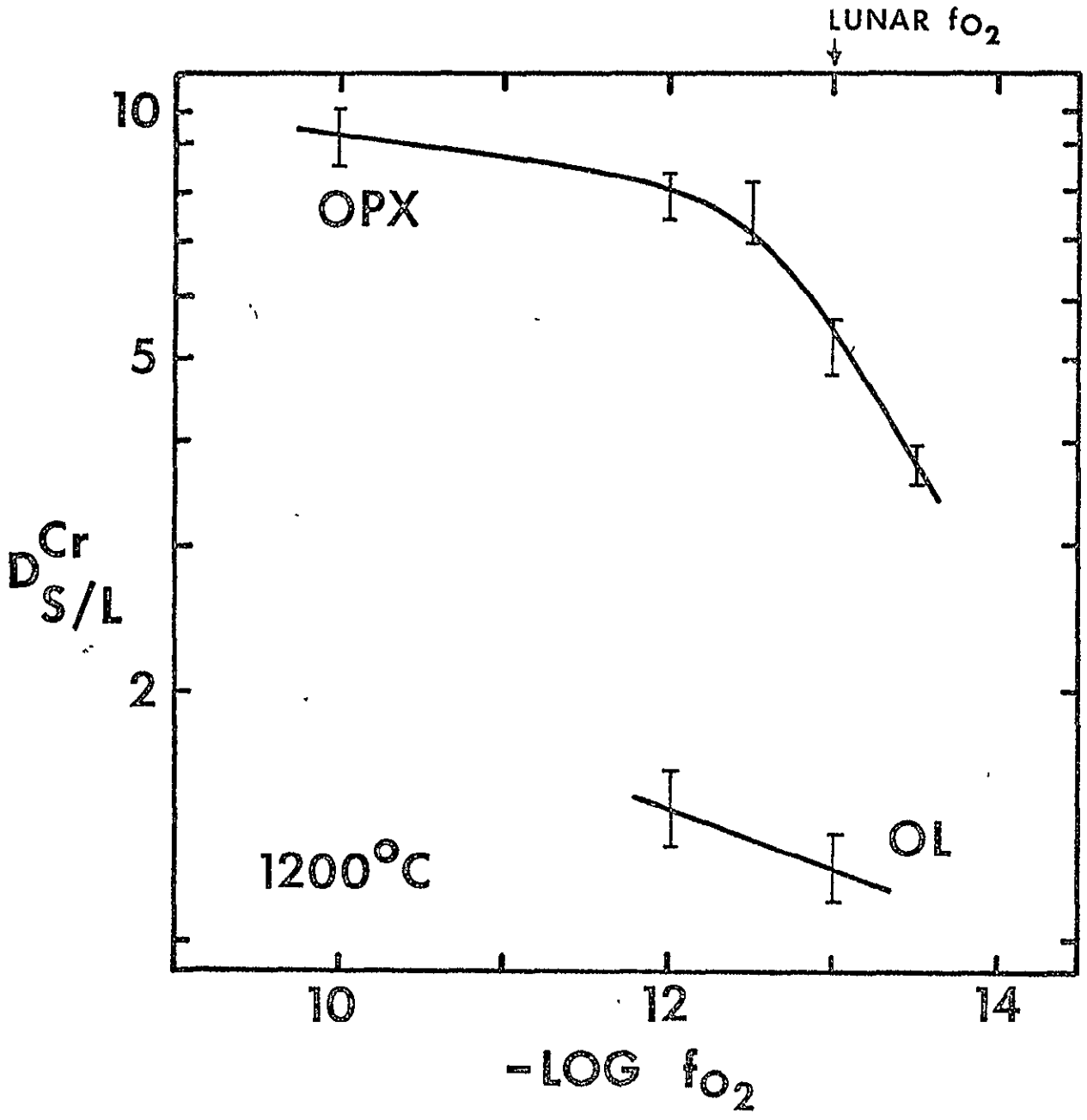

FIG.

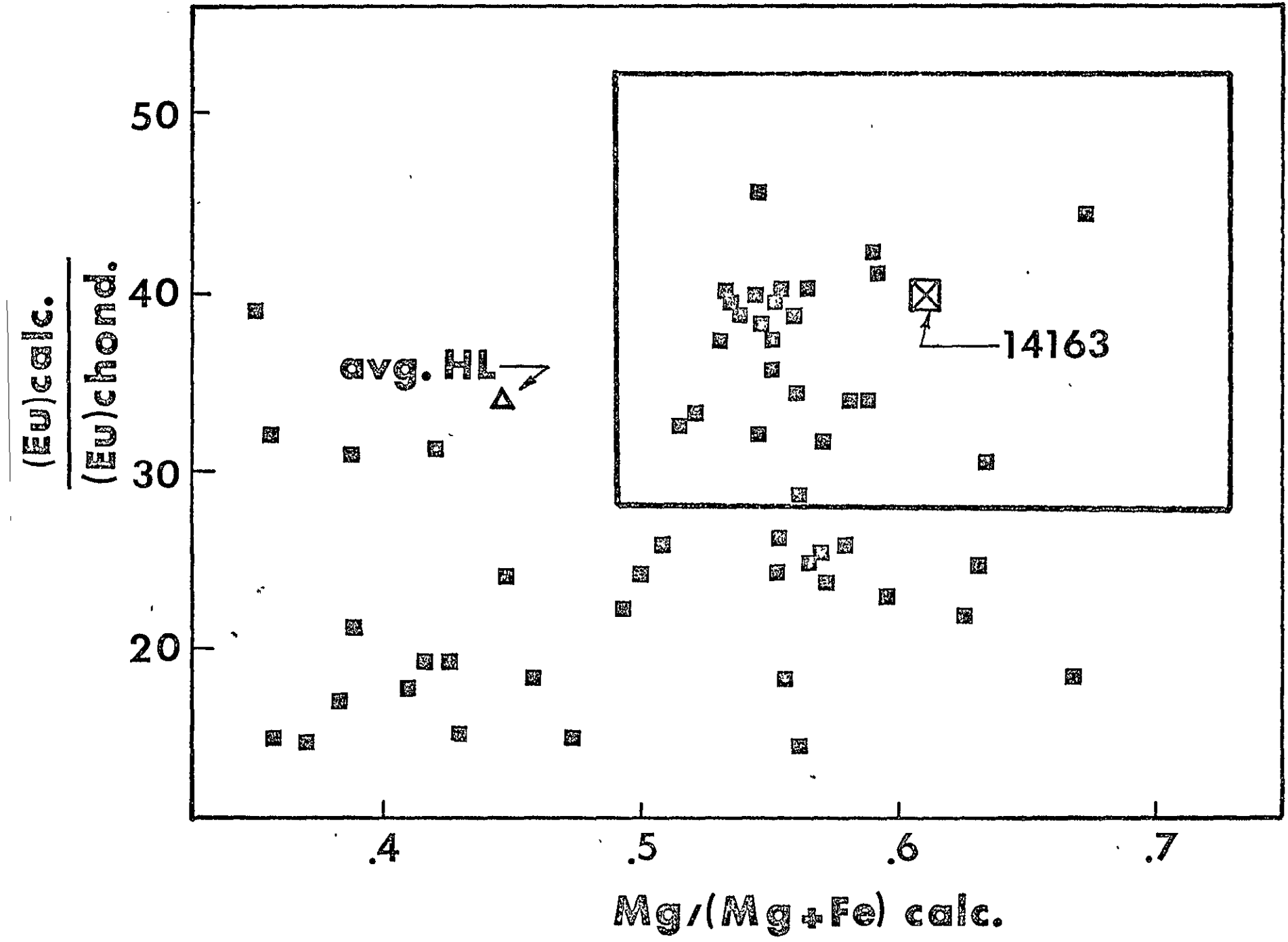

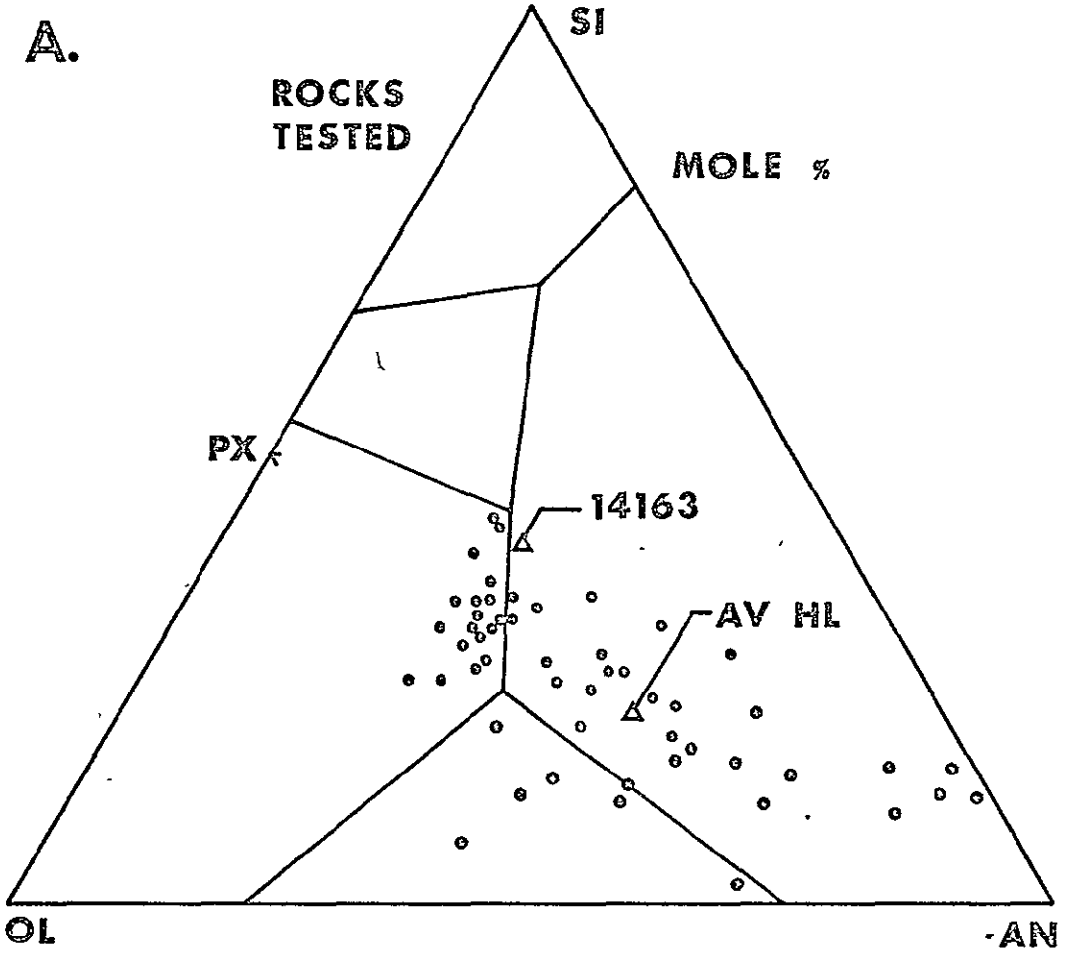
A.
ROCKS TESTED
SI
MOLE %
PX
14163
AV HL
OL
AN

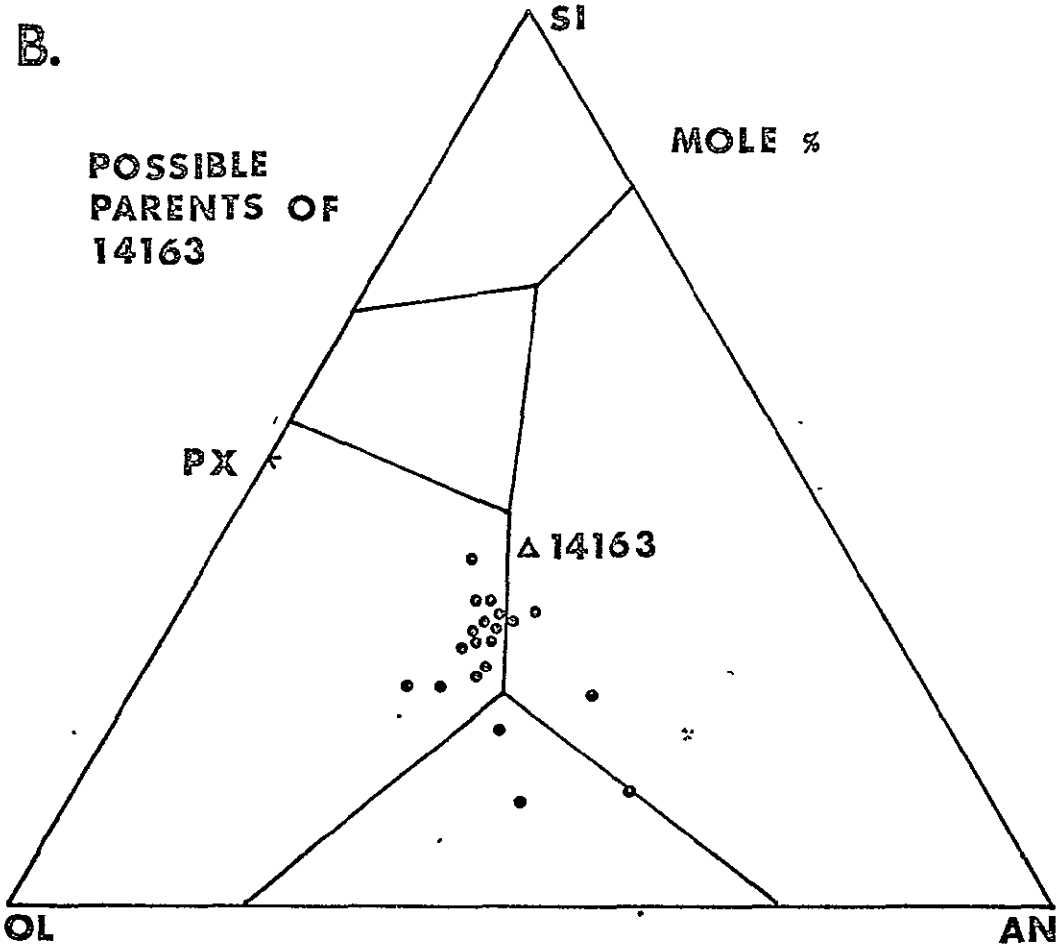
B.
POSSIBLE PARENTS OF 14163
SI
MOLE %
PX
14163
OL
AN

FIG. 5

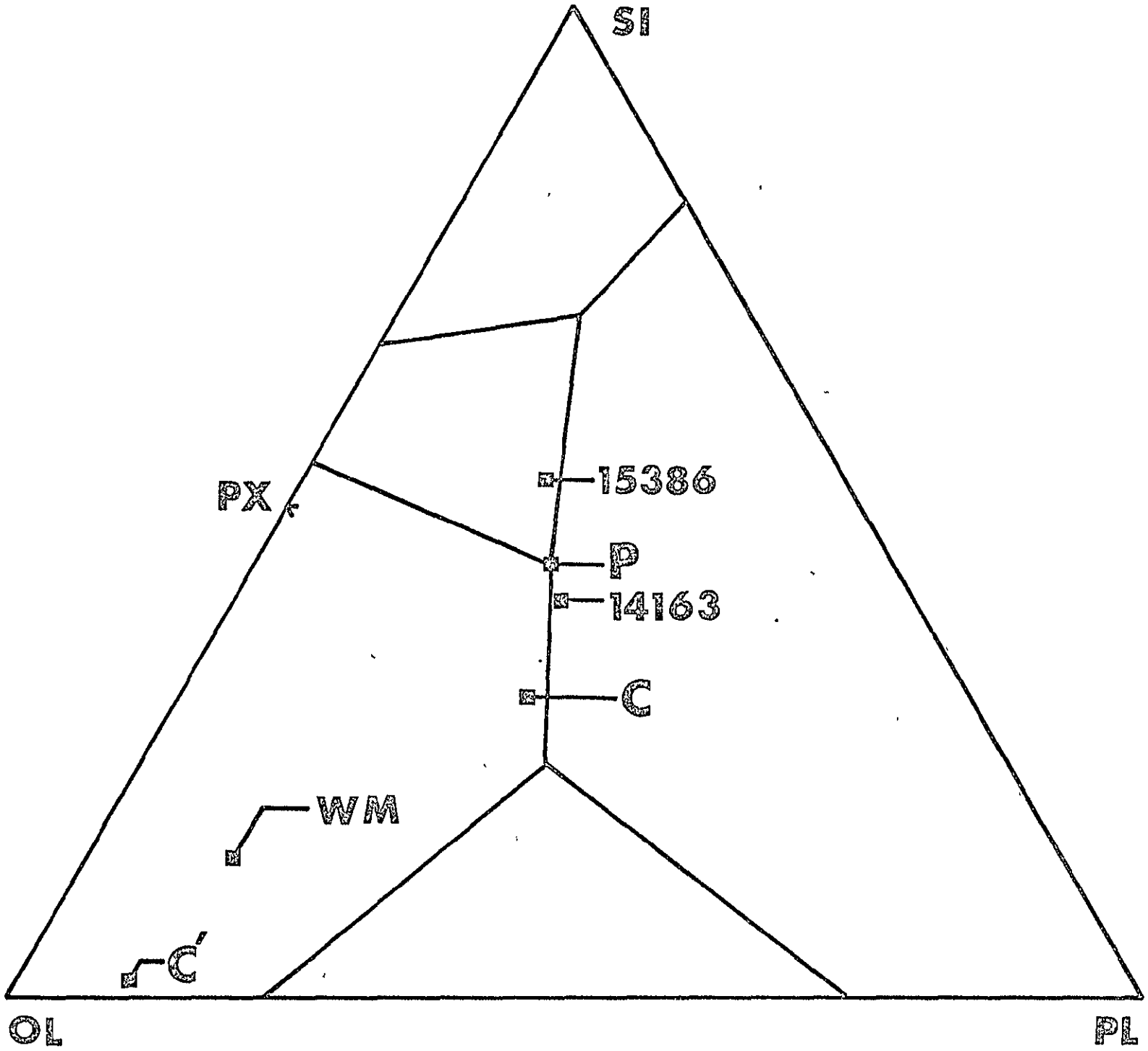

FIG. 6

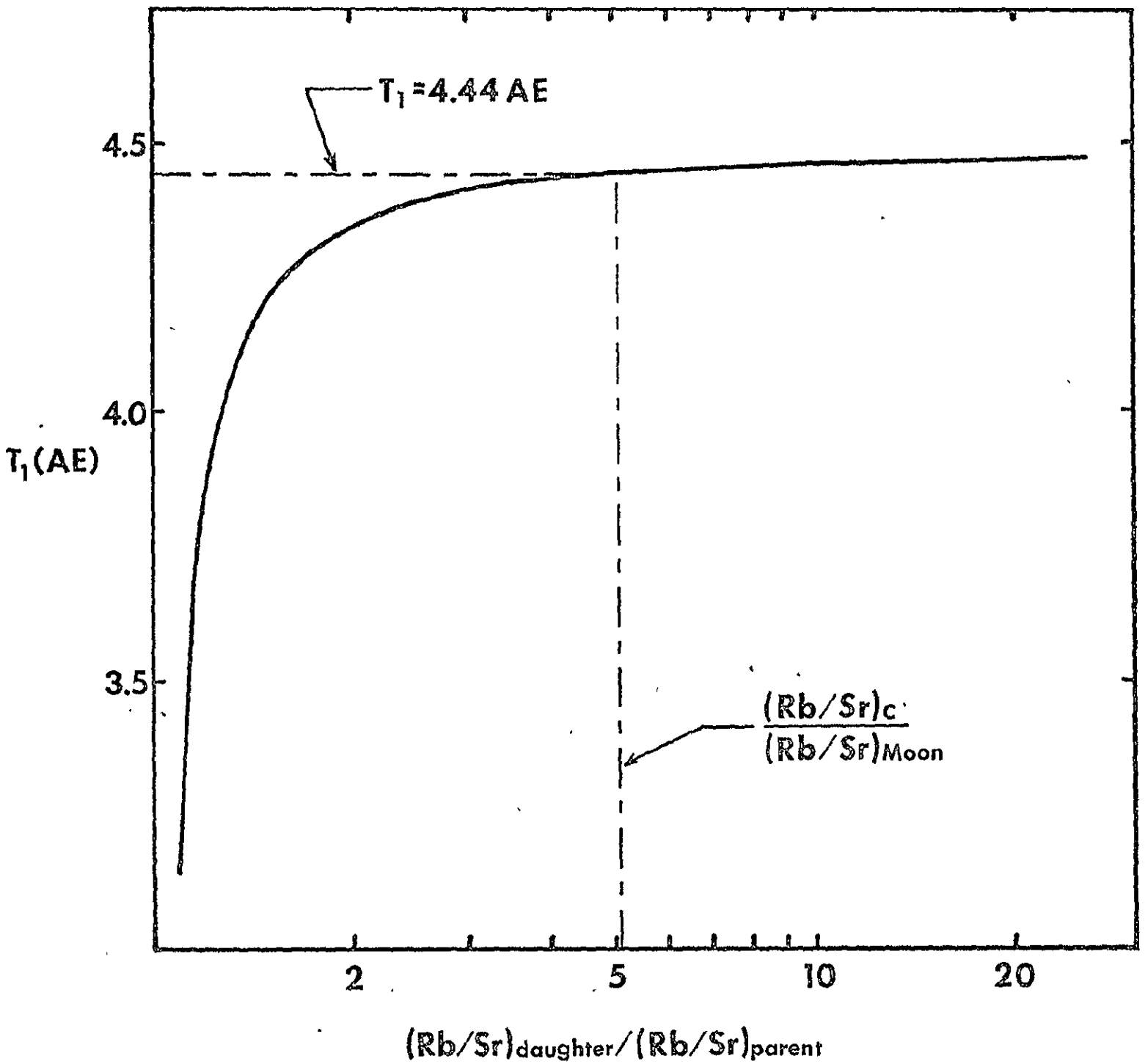
T_1 = 4.44 AE
4.5
4.0
3.5
T_1 (AE)
$\frac{(Rb/Sr)_c}{(Rb/Sr)_{Moon}}$
2
5
10
20
$(Rb/Sr)_{daughter}/(Rb/Sr)_{parent}$

FIG. 7

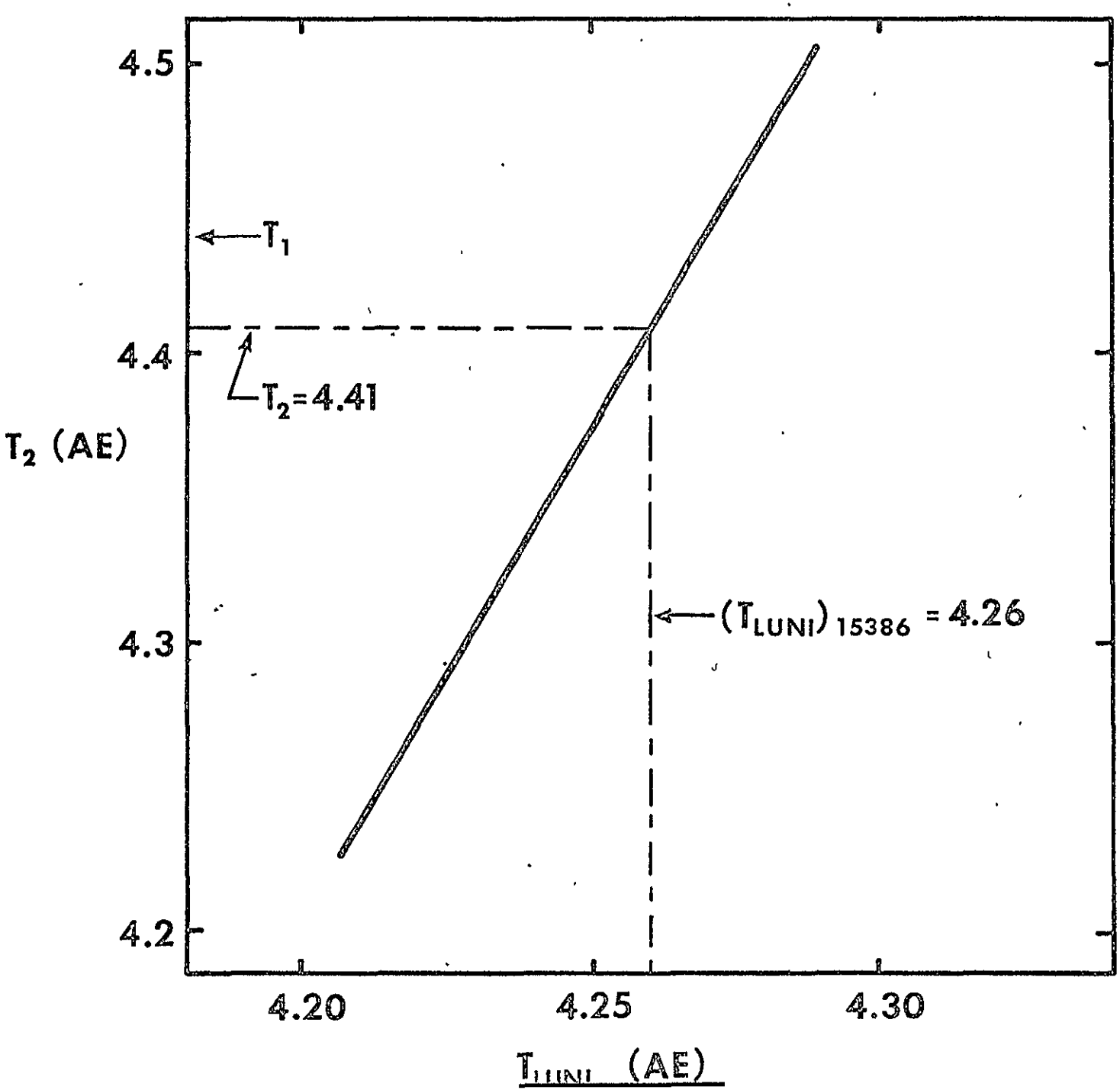

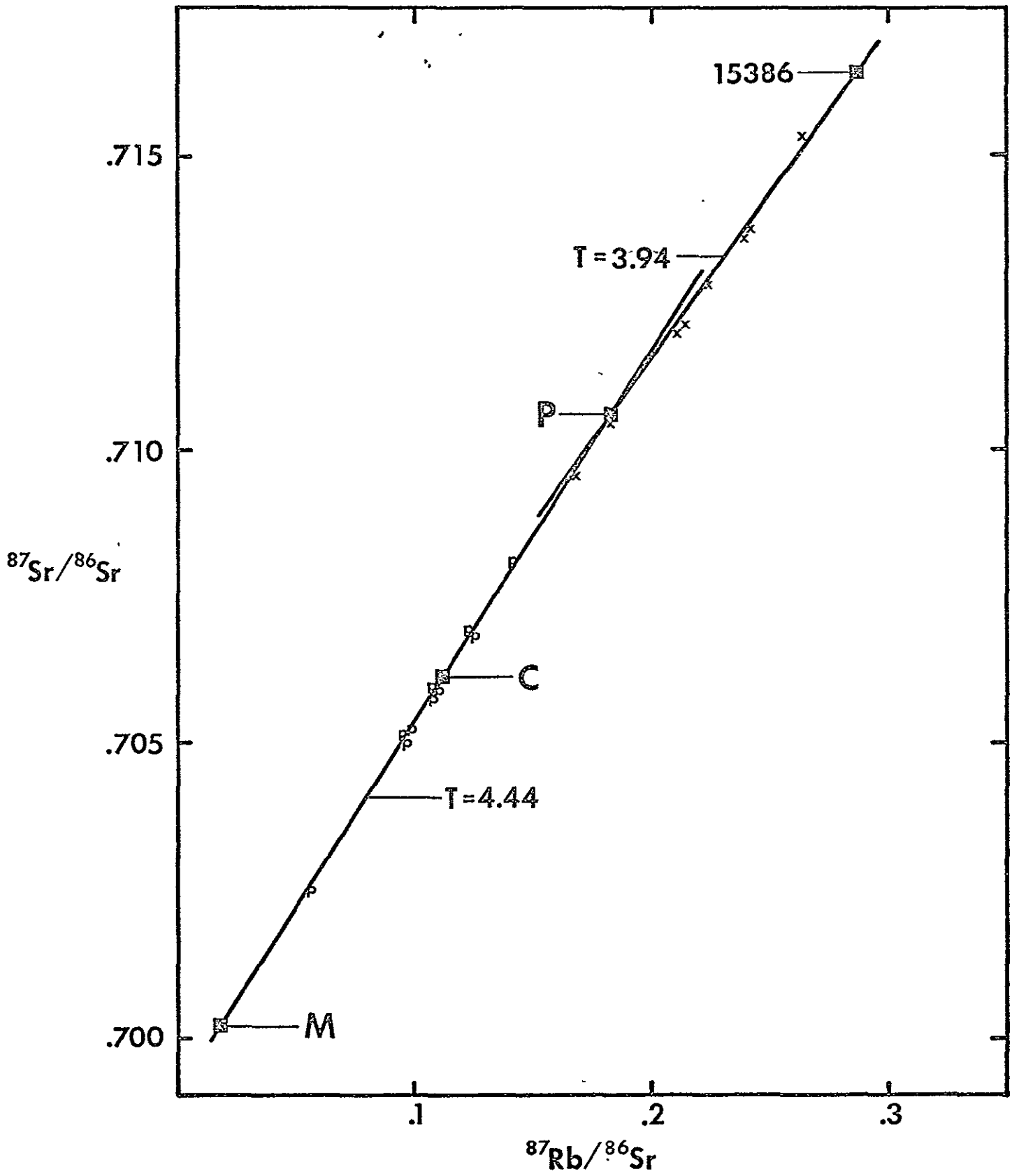
15386
T = 3.94
P
C
T = 4.44
M
.715
.710
.705
.700
.1
.2
.3
$^{87}Sr/^{86}Sr$
$^{87}Rb/^{86}Sr$

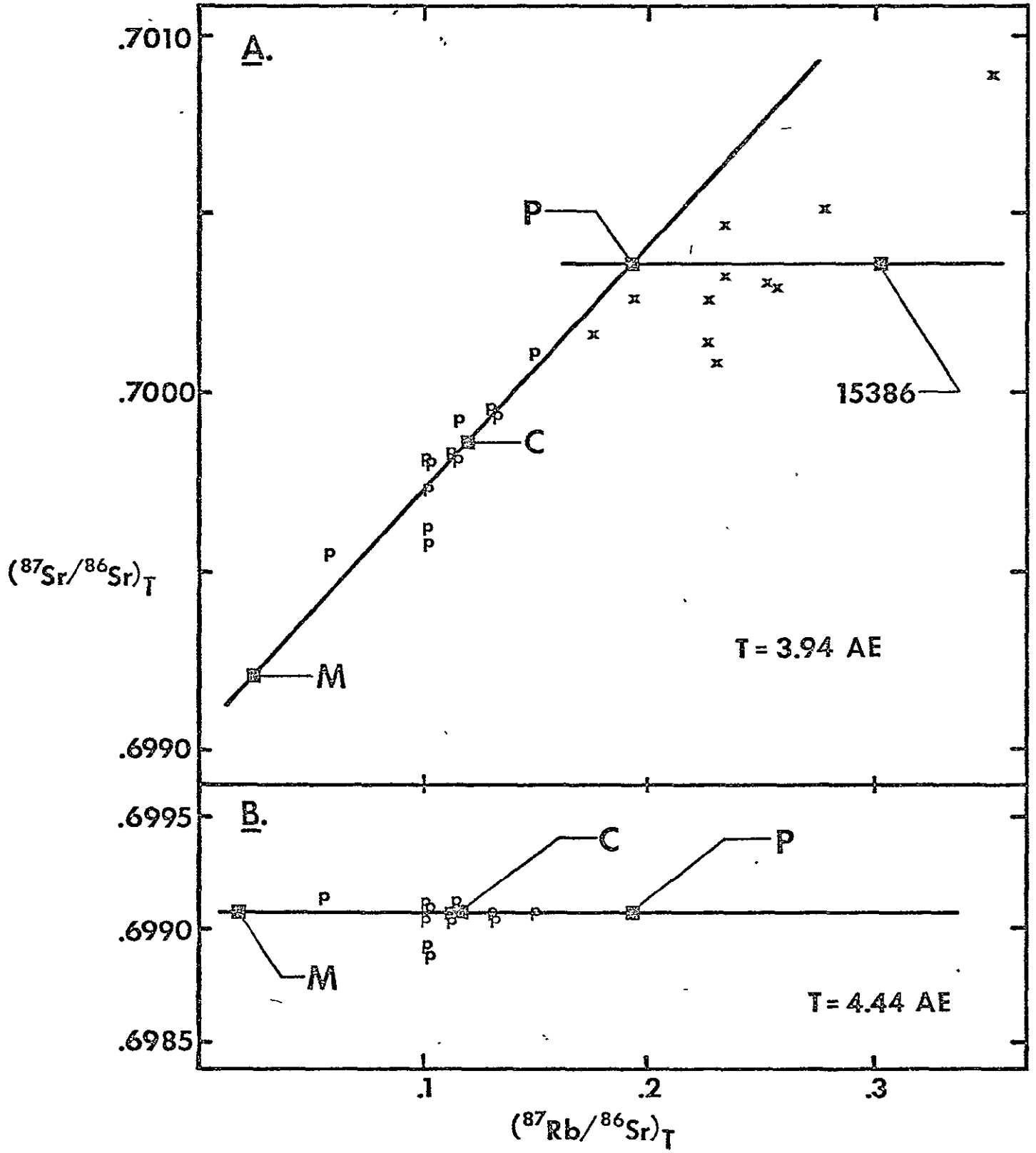
A.
.7010
.7000
.6990
P
C
M
15386
T = 3.94 AE
B.
.6995
.6990
.6985
C
P
M
T = 4.44 AE
.1
.2
.3
$(^{87}Sr/^{86}Sr)_T$
$(^{87}Rb/^{86}Sr)_T$

McKay and Weill
6/16/76

FIG. 10

A MODEL FOR KREEP PETROGENESIS

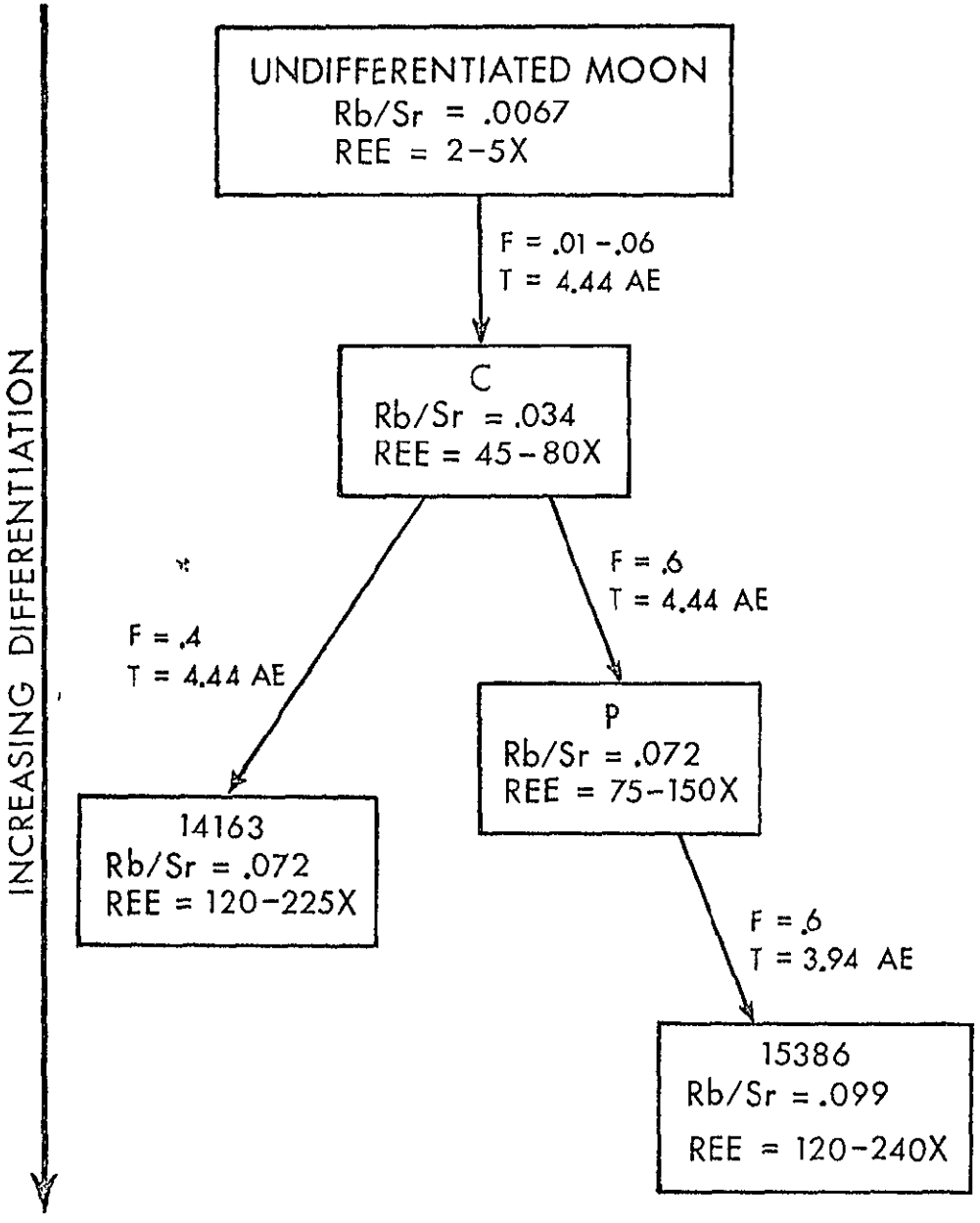

FORMATION OF C (=LKFM?) FROM PRIMITIVE MATERIAL THROUGH FRACTIONATION OF LARGE AMOUNTS OF OLIVINE + LESSER AMOUNTS OF PLAGIOCLASE + ?

DIFFERENTIATION OF C DURING THE SAME IGNEOUS EPISODE IN WHICH IT WAS FORMED, PRODUCING A SUITE OF MORE EVOLVED KREEP ROCKS INCLUDING P AND 14163.

DIFFERENTIATION OF P TO FORM VERY HIGHLY EVOLVED COMPOSITIONS IN A LATER IGNEOUS EVENT.

Proc Lunar Sci Conf 6th (1975), p 1143–1158
Printed in the United States of America

The partitioning of Mg, Fe, Sr, Ce, Sm, Eu, and Yb in lunar igneous systems and a possible origin of KREEP by equilibrium partial melting

D. F. WEILL and G A MCKAY

Department of Geology, University of Oregon, Eugene, Oregon 97403

Abstract—The solid/liquid distribution of Mg, Fe, Sr, Ce, Sm, Eu, and Yb have been determined over crystallization paths in the system $(Mg, Fe)_2SiO_4$–SiO_2–$CaAl_2Si_2O_8$ Varying degrees (1–5 wt %) of partial melting of an olivine + orthopyroxene + plagioclase rock yield liquids with large-iron lithophile (LIL) and major-element concentrations strikingly similar to those of some Apollo 15 and 16 KREEP rocks The parent assemblages from which these KREEP melts can be derived have a bulk composition similar to that previously proposed for the whole moon Partial melts derived from a source with the same mineralogy but with a chemical composition corresponding to the average lunar highland do not simultaneously satisfy the major-element and LIL concentration characteristics of KREEP

INTRODUCTION

THE DIFFERENCES OF CHEMICAL COMPOSITION observed in lunar rocks can either be attributed to heterogeneities associated with the original accretion of the moon or to subsequent large scale solid–liquid phase separation processes Geochemical arguments (Brett, 1973, Duncan *et al.*, 1973; Taylor and Jakeš, 1974) indicate a relatively homogeneous accretion. Furthermore, rapid accretion (Mizutani, 1972) could have resulted in an early liquid outer shell extending to a depth of at least several hundred kilometers. Cooling and crystallization of this initial liquid shell would result in chemical differentiation that would have characteristics imposed by solid–liquid partitioning of the elements. Numerous models have been proposed to explain how an initial global igneous complex on the moon might account directly (or indirectly through subsequent internal partial melting) for the main rock types observed in the lunar sample collection Volcanism and large impacts on the lunar surface could have served to bring representative rock types or their partially molten derivatives to the surface It has also been proposed (Warner *et al.*, 1974) that surface impacts may themselves cause differentiation of the lunar crustal material via liquid–solid separation after impact melting.

In one form or another, almost all models for the geochemical evolution of the moon relate the main lunar rock types to each other via a relatively simple sequence of crystallization and/or partial melting processes One of the principal tests of such models is a verification of compositional trends by means of experimental crystallization studies Since both major- and trace-element concentrations in the lunar samples place critical constraints on the models, it is important that experimental verifications include data on both types of constituents. We have previously described some of the important factors to be considered in determining the evolution of elemental distributions during lunar

igneous differentiation processes (Weill *et al*, 1974) and applied them to the evolution of Sm (indicative of "typical" REE) and Eu ("anomalous" REE) concentrations during various postulated fractional crystallization and partial melting sequences in lunar igneous systems.

The solid/liquid distribution coefficients we employed for Sm and Eu (Weill and Drake, 1973; Sun *et al.*, 1974, Grutzeck *et al*, 1974; Drake and Weill, 1975) were necessarily approximate because they had been determined experimentally in systems which departed in composition from the lunar systems to which we applied them Furthermore, our postulated crystallization sequences were based entirely on the olivine–plagioclase–silica pseudoternary liquidus diagram (Walker *et al*, 1972, 1973) which does not contain any information about the interphase distribution of the major elements Mg and Fe Nevertheless, within the limits imposed by the data it was shown that the evolution of liquids with KREEP characteristics could most easily be accomplished by partial melting and that there was a rather tight mutual constraint between the assumed Sm and Eu abundances of the parent rock, the mineralogy of the refractory parent assemblage, and the degree of partial melting

We have now added to our experimental data base by (a) Directly determining the crystallization sequences of a molten average highland composition (Taylor and Jakeš, 1974) and a much more ferromagnesian liquid These experiments yield information on the distribution of the major elements, Mg and Fe, between olivine, orthopyroxene and coexisting liquids, and thus allow us to combine the constraints imposed by the evolution of these important major-element indicators with those imposed by the trace elements. (b) Directly measuring the solid/liquid distribution coefficients of the trace elements Sr, Ce, Sm, Eu, and Yb for plagioclase and orthopyroxene over the same crystallization sequences. This extends our data to five trace elements, including a control on the relative enrichment of light versus heavy REE Also, since the distribution coefficients have now been measured directly in the system to which the modeling will be applied, the compositional dependence is no longer a source of uncertainty.

In this paper we report the new experimental data, and we present an analysis of the possibility of generating KREEP-type liquids by one step partial melting or crystallization of systems with whole-moon abundances of LIL trace elements and a subsolidus mineralogy dominated by olivine, orthopyroxene, and plagioclase. We also discuss the plausibility of deriving KREEP-type liquids by impact melting differentiation of the average highland surface.

EXPERIMENTAL METHODS

The average highland (HL) and ferromagnesian (FMG) crystallization sequences were experimentally determined by holding the appropriate bulk compositions at temperature and oxygen fugacity (H_2 and CO_2 gas mixtures) in SiC resistance furnaces for periods of 24–48 hr Charges were held in Pt–Rh wire loops formed from 2.5×10^{-4}-m diameter wire which had been previously held in contact with the same molten composition at 1400°C and the I–W equilibrium oxygen fugacity for 48 hr The runs themselves were all carried out at oxygen fugacities for which the Fe^{3+}/Fe^{2+} in the liquid is negligible Compositions of the individual phases are based on a minimum of 10 point analyses per phase The

modes were determined from the bulk composition and the individual phase compositions by multilinear regression analysis After the liquid and solid compositions at various stages of the crystallization sequences were determined as described above, new experimental charges were prepared with a bulk composition equal to the liquid plus a small amount of plagioclase and/or pyroxene These compositions were doped with an additional 1–3 wt % of one of the LIL "trace" elements and held at temperature and oxygen fugacity for 100–150 hr After quenching, solid and glass were analyzed for the LIL element (distribution coefficient) and major constituents (to check that the major-element compositions of all phases were close to those determined previously for the crystallization sequence) In effect, the trace-element distribution coefficients are determined in bulk systems that lie slightly off the multiple saturation boundaries as depicted, say, in the ol–opx–plag pseudoternary liquidus system Each LIL and each solid–liquid pair is studied in a separate group of experiments in order to circumvent problems arising from excessive enrichment in "trace" elements and from working with liquid-poor, multiply-saturated systems Runs used to determine LIL trace element distribution coefficients were performed over a range of oxygen fugacities from "air" to two orders of magnitude below the I–W equilibrium curve Only the Eu plagioclase/liquid distribution coefficient exhibits significant dependence on oxygen fugacity

Experimental Results

The results of the experimental crystallization runs are given in Table 1 The Fe and Mg solid/liquid distribution coefficients for olivine and orthopyroxene are plotted against reciprocal temperature in Fig 1, and the linear regression coefficients are given in Table 2. Crystallization sequences for new bulk compositions can be calculated from the experimentally determined sequences, effectively stretching the applicability of the experimental set. For instance, the addition (or subtraction) of $CaAl_2Si_2O_8$ to bulk composition HL simply results in an equivalent increment of plagioclase at each step of the new crystallization sequence The addition of $(Mg, Fe)_2SiO_4$ to bulk composition FMG similarly results in additional olivine, but because of the Mg–Fe exchange between olivine, liquid, and orthopyroxene during equilibrium crystallization the new crystallization sequence can be approximately calculated only with a knowledge of the Mg and Fe distribution coefficients. In Table 3 we list a crystallization sequence calculated for a liquid with a bulk composition corresponding approximately to the liquid at 1380°C in the original FMG sequence (Table 1) plus 54 wt % of the olivine (Fo_{93}) with which this liquid is in equilibrium This calculated sequence is referred to as "FMG " Various aspects of the crystallization sequences HL and "FMG" are shown in Figs 2, 3, and 4

The distribution of Sr, Ce, Eu, Sm, and Yb between plagioclase, orthopyroxene, and liquid is shown in Table 4 These coefficients are valid for the solid–liquid pairs which approximate in composition the coexisting phases along the crystallization paths, i.e , near the boundary lines and reaction point of the olivine–plagioclase–silica pseudoternary system To the extent that their composition dependence is not pronounced within this ternary system they are roughly applicable to coexisting phases within it Notice that although the coefficients are given at two temperatures, both the temperature and composition dependence are inseparably incorporated in the data. Low-pressure melting of an olivine + plagioclase + orthopyroxene assemblage begins slightly below 1200°C, and the

Table 1 Experimental crystallization of average highland (HL) and ferromagnesian (FMG) composition liquids

T (°C)	Phase (wt %)	SiO_2	TiO_2	Al_2O_3	Cr_2O_3	FeO	MgO	CaO
1400	HL liq(100)	45 2	0 63	25 3	0 10	6 5	8 0	14 2
1320	liq (77)	45 7	0 78	22 2	0 14	8 3	10 3	12 6
	plag(23)	44 1	0 00	36 0	0 00	0 28	0 37	19 3
1280	liq(67)	45 8	0 87	20 4	0 11	9.4	11 7	11 8
	plag(33)	43 6	0 00	35 9	0 05	0 45	0.41	19 6
1260	liq(58)	46 4	1 10	18 9	0 15	10 5	11 8	11 2
	plag(40)	43 5	0 02	36 0	0 01	0 45	0 37	19 7
	ol(2)	40 5	0 00	0 26	0 10	12 2	46.4	0 58
1220	liq(38)	48 0	1 64	16 8	0 18	12 8	10 0	10 6
	plag(53)	44 2	0 02	35 5	0 02	0 43	0 41	19 4
	ol(9)	39.6	0 02	0 22	0.16	15 9	43 6	0 52
1200*	liq + plag + opx + ol							
1400	FMG liq(100)	51 1	0 31	11 85	0 22	9 23	21 1	6 1
1380	liq(93)	51 4	0 33	12 9	0 21	—	19 0	6.6
	ol(7)	42 1	0 00	0 01	0.12	5 9	51 6	0 24
1320	liq(79)	52 3	0 39	14 8	0 22	9 7	15.1	7 5
	ol(13)	41 2	0 00	0 07	0 17	8 7	49 6	0.26
	opx(8)	57.1	0 00	1 20	0 32	5 3	35 7	0 44
1280	liq(72)	52.0	0 42	16 1	0 19	9 7	13 4	8 3
	ol(13)	41 0	0 00	0.09	0.15	10 1	48 4	0 27
	opx(15)	56 1	0 03	1.93	0 45	6 5	34 2	0.78
1260	liq(61)	50 8	0 48	17 7	0 13	9.9	11 6	9 3
	ol(10)	40 6	0 00	0 06	0.11	11 3	47 7	0 24
	opx(29)	54 9	0 06	3 7	0 50	7.2	32 6	1.07
1240	liq(58)	50 2	0 50	17.9	0 10	10 3	11 3	9 8
	ol(6)	40 5	0.00	—	0 09	11 2	48 0	0 21
	opx(36)	55 0	0 08	4 0	0 48	7 1	32 3	1 11
1220	liq(54)	50 4	0 49	18 2	0 09	10 0	10 4	10.4
	ol(6)	40 7	0 00	0 06	0 08	12 4	46 5	0 28
	opx(40)	54 1	0 12	5 0	0 42	7 7	31.3	1 29
1200*	liq + ol + plag + opx							

*Low-quality analyses sufficient only for phase identification

Table 2 Solid/liquid (weight basis) distribution coefficients for Mg and Fe in olivine and orthopyroxene along the crystallization paths FMG and HL Coefficients in the equation, $\log_{10} D = A + B/T$, where T is in °K The Fe–Mg exchange coefficient as defined by Roeder and Emslie (1970), $K_D = (X^s_{Fe})(X^l_{Mg})/(X^l_{Fe})(X^s_{Mg})$, is equivalent to D_{Fe}/D_{Mg}

Solid	Element	A	B
Olivine	Mg	−1 451	3138
Olivine	Fe	−1 960	3067
Orthopyroxene	Mg	−1 232	2557
Orthopyroxene	Fe	−2 269	3225

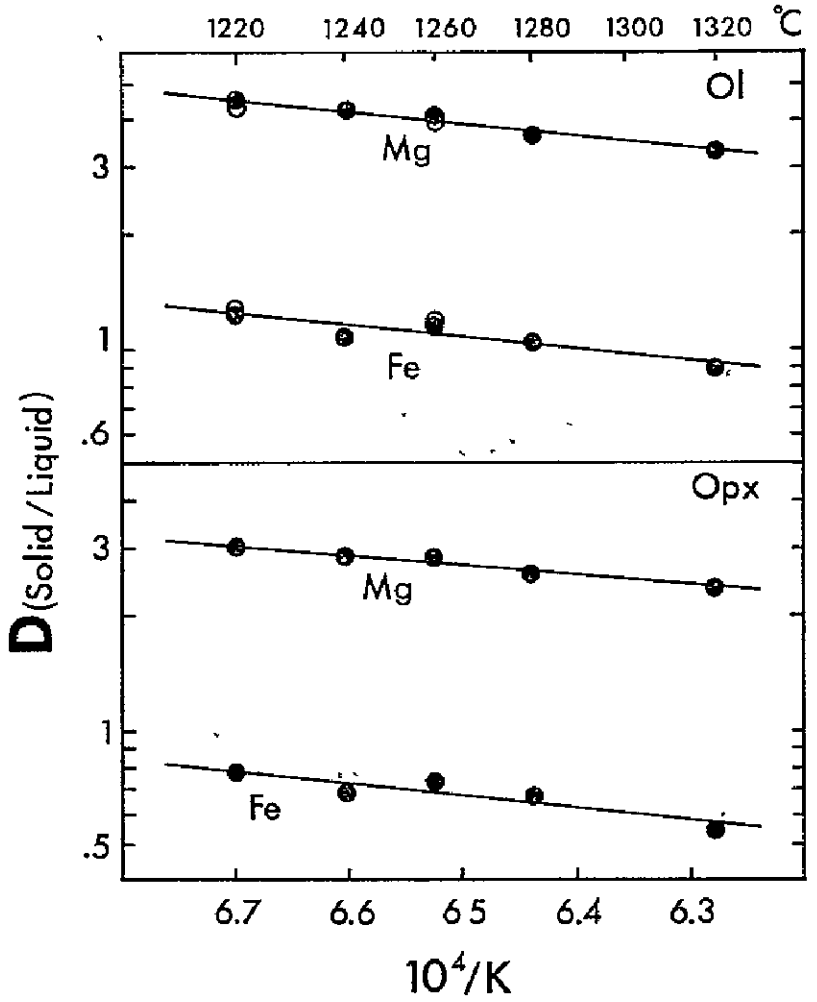

Fig 1 Fe and Mg distribution coefficients (weight basis) Open circles represent data from charges of bulk composition HL, closed circles from composition FMG Linear regression coefficients are given in Table 2

melt does not vary greatly in composition provided the degree of partial melting is not large Consequently, in considering the partitioning of these trace elements between a partial melt and a refractory residue containing plagioclase and orthopyroxene, the coefficient values at 1200°C are representative It can be seen that plagioclase preferentially incorporates the light versus the heavy REE while orthopyroxene discriminates even more strongly in favor of the heavy REE

Orthopyroxene displays very little potential for creating anomalous Eu abundances. In Fig 5 we have plotted the variation of the Eu distribution between plagioclase and liquid as a function of oxygen fugacity, showing the very large potential for anomalous Eu abundances developed in plagioclase under strongly reducing conditions. The coefficients corresponding to lunar oxygen fugacities

Table 3 Calculated crystallization sequence "FMG."

T (°C)	Phase (wt %)	SiO_2	Al_2O_3	FeO	MgO	CaO
?	liq(100)	48 8	8 6	8 4	30 0	4 4
?	liq(80)	50 5	10 7	9 0	24 4	5 4
	ol(20)	41 5	0 0	5 8	52 5	0 3
1380	liq(65)	52 7	13 2	9 1	18 4	6 6
	ol(35)	41 3	0 0	7 1	51 4	0 3
1320	liq(55)	52 8	15 5	8 9	15 1	7 8
	ol(38)	41 1	0 0	8 2	50 5	0 3
	opx(7)	57 5	1 2	5 1	35 8	0 4
1280	liq(50)	52 5	16 7	8 6	13 8	8 4
	ol(37)	40 9	0 0	9 0	49 9	0 3
	opx(13)	56.8	1 9	5 6	35 0	0 8
1260	liq(43)	52 1	18 3	8 6	11.6	9 5
	ol(37)	40 8	0 0	9 5	49 4	0 3
	opx(20)	55 5	3 5	6 0	34 0	1 0
1240	liq(40)	51 9	19 2	8 3	10 5	10 1
	ol(36)	40 7	0 0	9 9	49 1	0 3
	opx(24)	55 2	3 8	6 3	33.7	1 1
1220	liq(38)	52 3	19 4	8 0	9 9	10 5
	ol(36)	40 7	0 0	10 2	48 9	0 3
	opx(26)	54 5	4 7	6 5	33 1	1 2
~1190	ol + opx + plag					

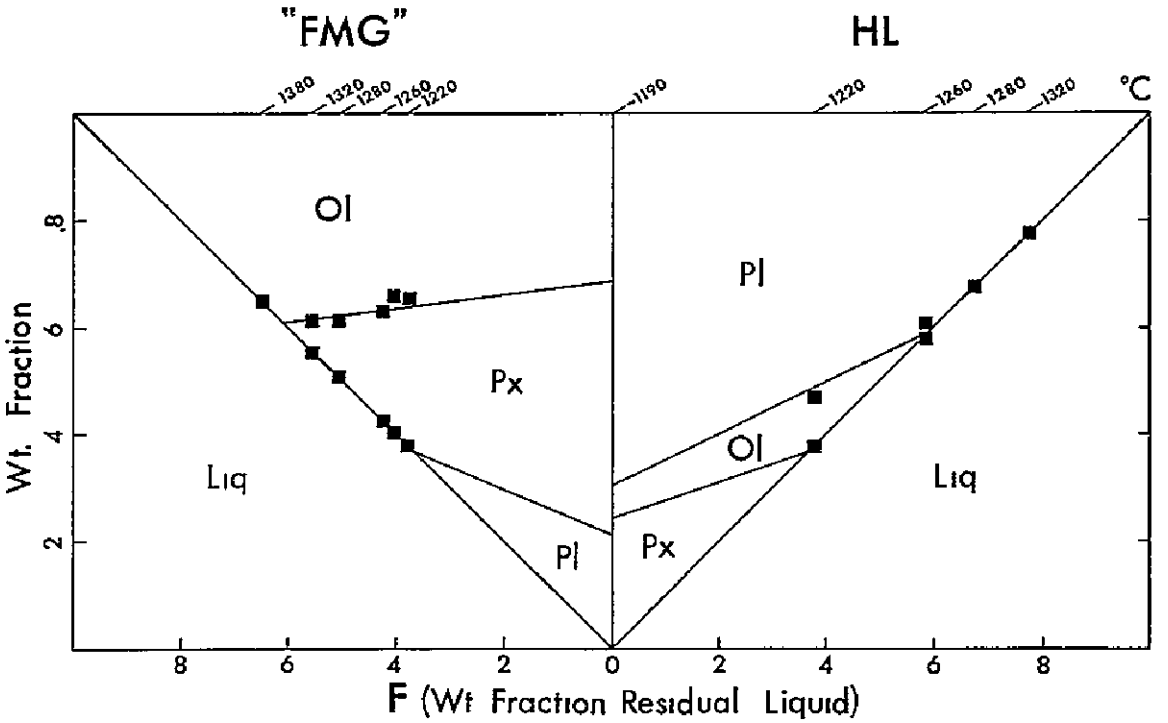

Fig 2 Phase assemblages (weight fractions) during equilibrium crystallization sequences HL and "FMG" Assemblages at $F = 0$ correspond to the normative proportions for the bulk compositions, with Fe and Mg partitioned between olivine and orthopyroxene according to the distribution coefficients in Fig 1

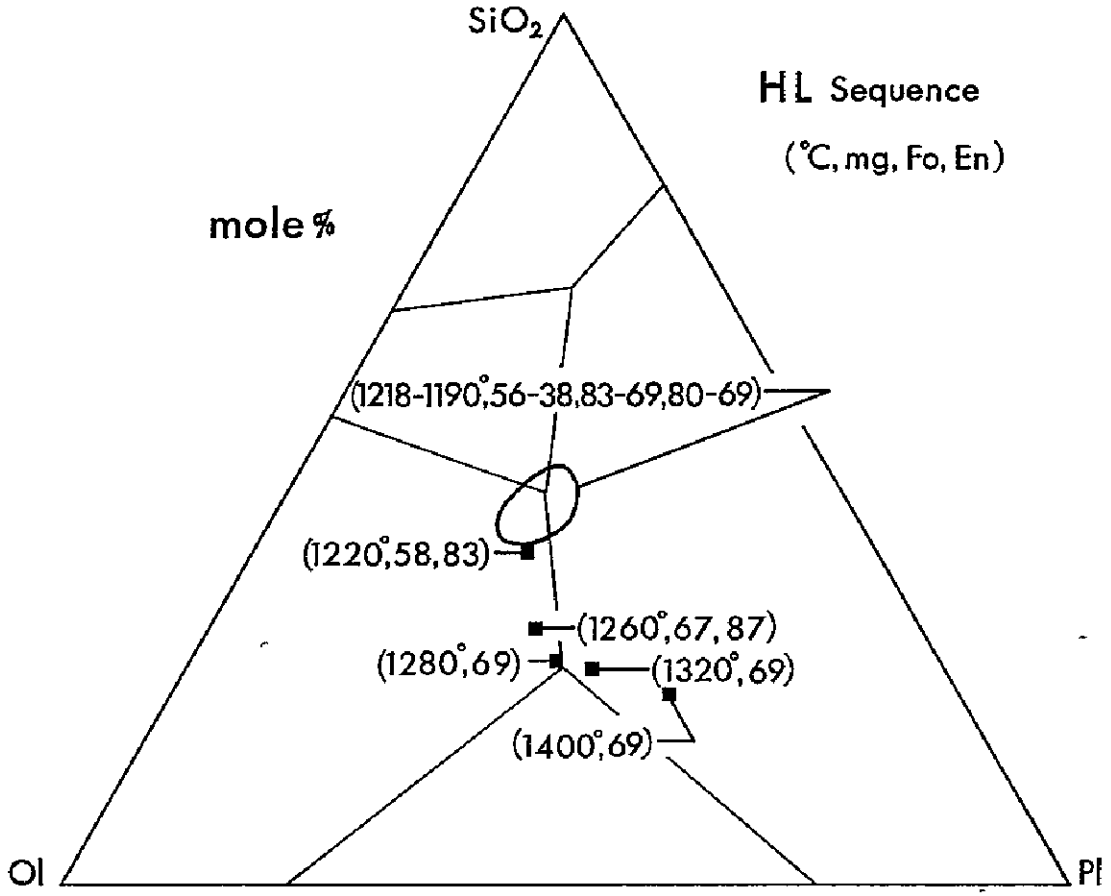

Fig 3 Equilibrium crystallization path in the pseudoternary system $(Mg, Fe)_2SiO_4$–SiO_2–$CaAl_2Si_2O_8$ for bulk composition HL Multiple-saturation curves of Walker *et al* (1973) are given for reference For each data point the temperature, *mg* value of the liquid, and the Fo and En contents of any coexisting olivine and orthopyroxene are given Crystallization below 1220°C leads the liquid to the four-phase peritectic "point," where crystallization proceeds (along with dissolution of olivine) to completion The exact location of the end point varies with the *mg* value and the minor-element content of the bulk composition, but lies within the indicated envelope The *mg*, Fo, and En at the end of crystallization were calculated using the distribution coefficients in Fig 1

Table 4 Plagioclase/liquid and orthopyroxene/liquid distribution coefficients for Sr, Ce, Sm, Eu, and Yb

	Plagioclase						Orthopyroxene					
	1340°C			1200°C			1340°C			1200°C		
	D	s_m	n	D	s_m	n	D	s_m	n	D	s_m	n
Sr	1 53	02	6	1 63	06	4	0 009	.006	2	0 018	003	3
Ce	0 062	002	5	048	001	5	0 006	002	3	0 009	002	5
Sm	0 044	002	10	032	002	10	0 013	005	2	0 022	001	9
Eu	1 1*	—	—	1 0*	—	—	0 014	003	3	0 022	002	7
Yb	0 031	002	10	0 028	003	6	0 056	010	2	0 170	010	6

*cf Fig 5

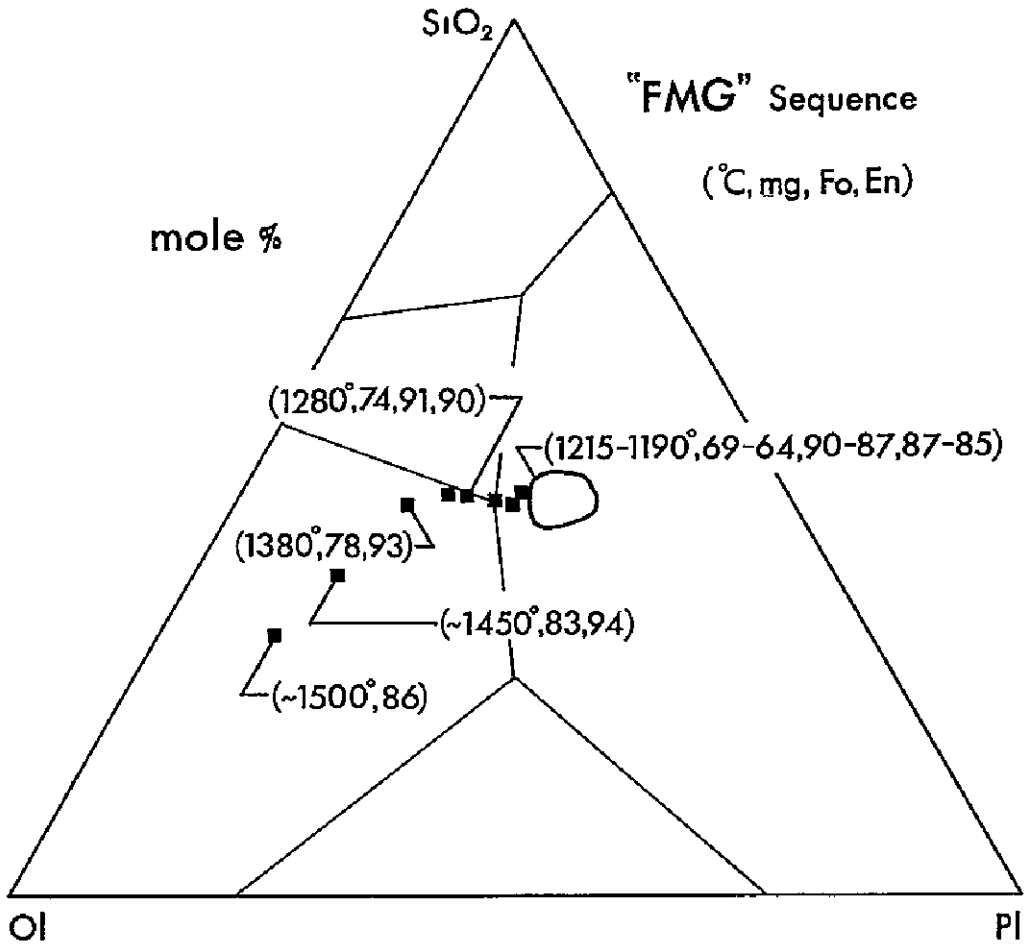

Fig 4 Calculated equilibrium crystallization path for bulk composition "FMG " Symbols same as in Fig 3

(Weill *et al* , 1974) have been incorporated in Table 4. The differences between the present set of plagioclase/liquid distribution coefficients and those determined by Drake and Weill (1975) are illustrated in Fig 6 These differences are indicative of the variation in the coefficients to be expected as a result of compositional variations in the two host phases (lunar "olivine–plagioclase–silica" liquids versus terrestrial andesites and andesitic basalts, and An_{100} versus An_{35}–An_{85} plagioclase).

DISCUSSION

The crystallization of HL and FMG liquids are seen in Figs. 3 and 4 to conform quite closely to the predictions based on the olivine–plagioclase–silica pseudoternary This may be interpreted as one more confirmation that the pseudoternary diagram is a realistic approximation in the sense that the primary crystallization "fields," three-phase "boundaries," and four-phase "points" are useful references for approximating phase proportions and compositions (with the exception of MgO and FeO) These exceptions turn out to be of interest in discussing the

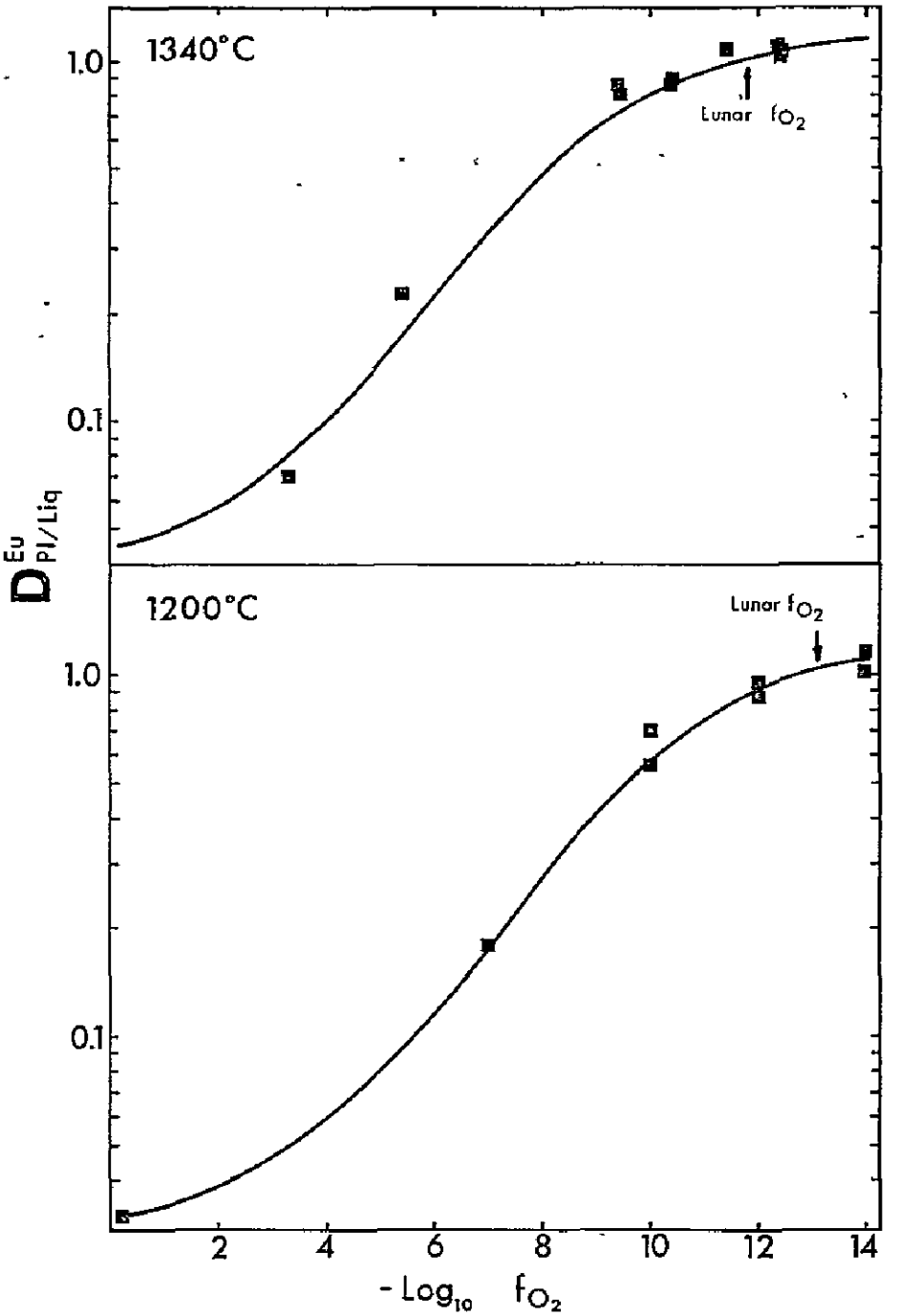

Fig 5 Variation of D_{Eu} for plagioclase/liquid with oxygen fugacity

possible origins of KREEP compositions by either partial melting or near-equilibrium crystallization. The major-element compositions of KREEP rocks typically plot in the area around the reaction "point" where the liquid is multiply saturated with olivine, orthopyroxene, and plagioclase This is compatible with an origin of KREEP by relatively low degrees of partial melting as pointed out by Walker *et al* (1972). KREEP has relatively "primitive" *mg* values (*mg* =

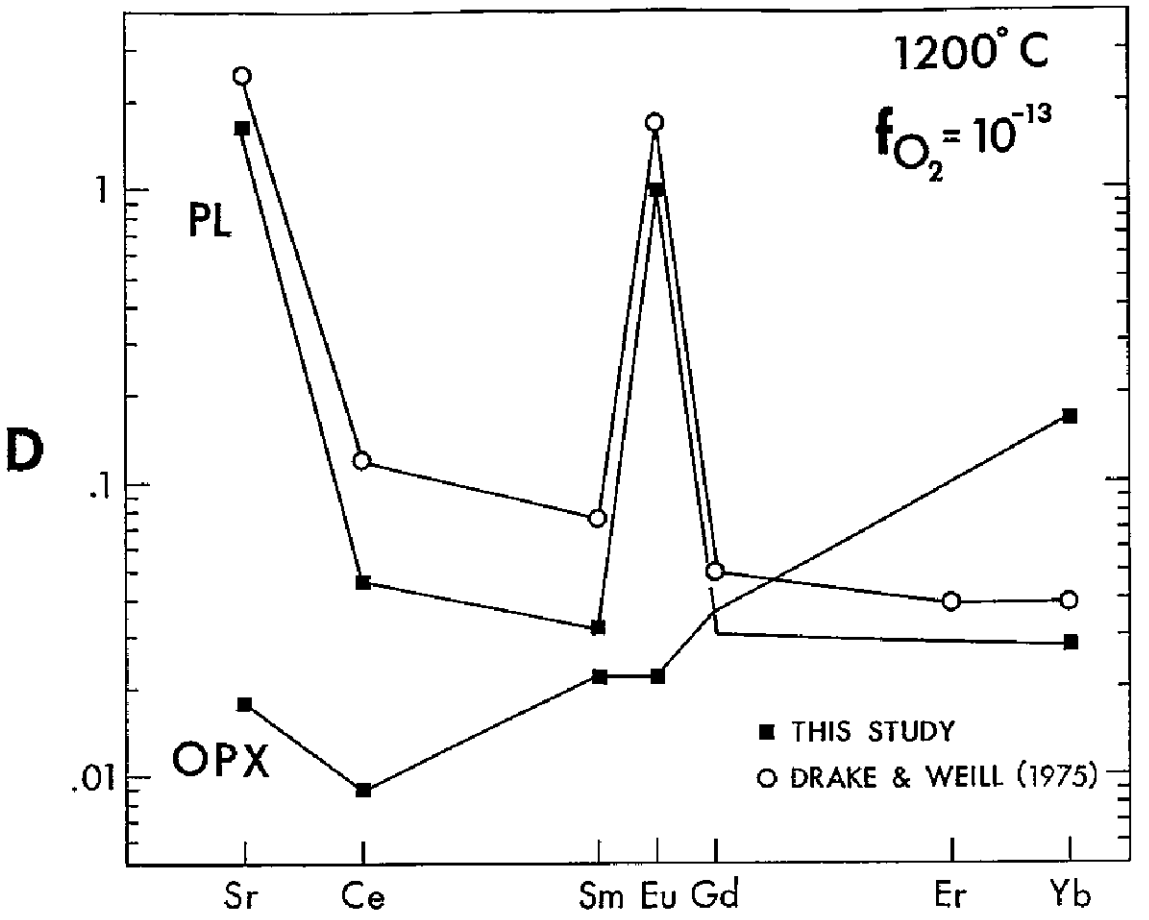

Fig 6 Plagioclase/liquid and orthopyroxene/liquid distribution coefficients Coefficients determined by Drake and Weill (1975) in terrestrial basaltic andesites are shown for comparison

100 Mg/(Mg+Fe), atomic basis). The relatively primitive *mg* and the highly differentiated LIL abundances are part of the puzzle of KREEP. The extensive fractional crystallization or very low degree of partial melting required to achieve the LIL enrichment have been considered likely to produce *mg* values too low to be compatible with KREEP In Table 5 we list analytical data for three Apollo 16 (*mg* = 69, 65, 66) and one Apollo 15 (*mg* = 58) KREEP-type rocks Referring to Figs. 2 and 3 we see that for the HL sequence this range of *mg* values is encountered only with a relatively large fraction of melt (> 30 wt %) such that the resulting enrichment (liquid/average highland) in the LIL elements would be far short of those typical of KREEP. This seems to be a problem in interpreting KREEP as the product of impact melting induced differentiation of the highland surface (Warner *et al.*, 1974) Referring to Figs. 2 and 4 we see that the partial melting of a more mafic material as typified by "FMG" would produce the correct major element concentrations (i e in the vicinity of the pseudo reaction point *and* with suitably high *mg* values) at low degrees of partial melting Some of the problems associated with producing KREEP by partial melting of plagioclase-rich

Table 5 Partial analyses of KREEP rocks Sources Hubbard *et al* (1973), Rhodes and Hubbard (1973), Hubbard *et al* (1974), Wiesmann and Hubbard (1975)

Wt %	64815	62235	65015	15386
SiO_2	47 0	47 1	47 2	50 8
Al_2O_3	17 6	18 9	23 2	14 8
FeO	9 5	9 4	8 7	10 6
MgO	11 6	10 0	9 5	8 2
CaO	11 9	11 5	10 1	9 7
ppm				
Sr	144	161	164	187
Ce	93 7	153	125	211
Sm	17 6	27 1	22 2	37 5
Eu	1 68	2 03	1 91	2 72
Yb	12 6	18 7	15 3	24 4
mg	69	65	66	58

rocks were previously discussed in terms of Sm and Eu abundances (Weill *et al.*, 1974) Briefly, it was pointed out that a high concentration of plagioclase in the refractory residue (e g as in the highland surface) results in excessive Eu depletion relative to the overall enrichment in REE (e g Sm) found in KREEP The results discussed above tend to confirm the unsuitability of HL as a parent material in terms of some of the major-element requirements of KREEP.

In the last analysis (no doomsday pun intended) all geochemical tests of models for the origin of lunar rock types such as KREEP reduce to plausibility arguments It must be admitted, however, that there is some arbitrariness about the selection of an *ad hoc* "FMG" composition which then "turns out" to be compatible with a KREEP partial melt Consequently, we must refrain from claiming too much for it, and simply be content to say that, if KREEP was formed by a one-step, near-equilibrium partial melting process, a parent material similar to "FMG" is not ruled out, while one such as HL is.

With a knowledge of the distribution coefficients for five trace elements (and a few assumptions) it turns out that we can approach the problem in a more systematic way. If we assume that partial melting of a mineral assemblage dominantly composed of olivine, orthopyroxene, and plagioclase is the origin of KREEP, the distribution coefficients can be used to test whether this is possible and, if so, to calculate the refractory assemblage in terms of the proportions of the minerals Obviously, we must also assume that melting occurs at sufficiently modest pressures so that the experimental distribution coefficients, obtained at atmospheric pressure, are representative. Rough estimates of the differences in partial molar volumes (solid versus liquid) for the trace elements in question do not indicate any unusually strong pressure dependence. It would be nice to know the pressure dependence of the distribution coefficients, but, in the meantime, it seems reasonable to assume that they will not change greatly at a few kilobars.

The relative values (even more critical) should hold to even higher pressures

The problem is best approached by considering the simple mass-balance for a trace-element partitioned between a partial melt and olivine, orthopyroxene, and plagioclase:

$$\bar{D} = D_{ol}W_{ol} + D_{opx}W_{opx} + D_{pl}W_{pl} = (C_o - C_L F)/(1-F)C_L,$$

where $\bar{D}$ is the composite solid/liquid distribution coefficient, C_o is the bulk system concentration, C_L is the concentration in the melt (KREEP), F is the mass fraction of liquid, and W_{ol}, W_{opx}, and W_{pl} are the mass fractions of the minerals normalized to a sum of unity. The models we present assume C_o to be equal to 7 × chondritic abundances, and C_L is set equal to the concentration in a particular KREEP rock. We consider that partial melting occurs at a temperature of approximately 1190°C and D_{opx} and D_{pl} are taken from the data in Table 4 extrapolated slightly from 1200°C to 1190°C. D_{ol} for all the LIL elements in question is assumed to be negligible (< 0.01) At any selected degree of partial melting (F) the above equation is linear in two independent variables (2 out of the 3W's). With five constraining trace elements we can obtain the best solution with a multilinear regression analysis at each selected value of F. A typical result of this procedure is shown in Fig. 7 where we plot the quality of the solution (r.m.s.d. between calculated and assumed $\bar{D}$) against F A best-fit for rock 64815 is clearly indicated at $F = 05$. An element-by-element comparison of the calculated partial melt with 64815 is illustrated in Fig 9 on the familiar abundance pattern plot The mode of the refractory residue (i.e. W_{ol}, W_{opx}, and W_{pl}) is plotted in Fig 8. The best solutions for other Apollo 16 KREEP-rich rocks, 62235 and 65015, are very similar, and, for these, we show only the calculated refractory modes in Fig 8. Apollo 15 rock 15386 is another, and perhaps better candidate for igneous KREEP, and the best solution for this rock ($F = .01$) is shown in Figs. 8 and 9. The refractory modes (approximately equivalent to the parent material for low degrees of partial melting) cluster rather tightly, indicating that these four KREEP partial melts could be produced by different degrees of partial melting of essentially the same parent rock type The proportions of plagioclase in the preferred parents (20–30 wt.%) is slightly greater than that previously deduced solely on the basis of Sm and Eu abundances (Weill *et al.*, 1974). The difference is in part due to the use of somewhat different distribution coefficients As previously discussed, the present set is more appropriate

The above approach can also be used assuming that the LIL concentrations in the KREEP source are equal to those of the average highlands (Taylor and Jakeš, 1974) As expected from our previous discussion of the HL composition, the resulting solutions yield parent materials that differ substantially from the average highlands in mg values.

We have assumed LIL concentrations in the KREEP source that are not greatly different from recent estimates for the whole moon (Taylor and Jakeš, 1974), but we have assumed nothing about the relative proportions of minerals in the source Therefore, it is interesting, and not a product of circular reasoning, that this mineralogy results in a major-element composition that resembles some

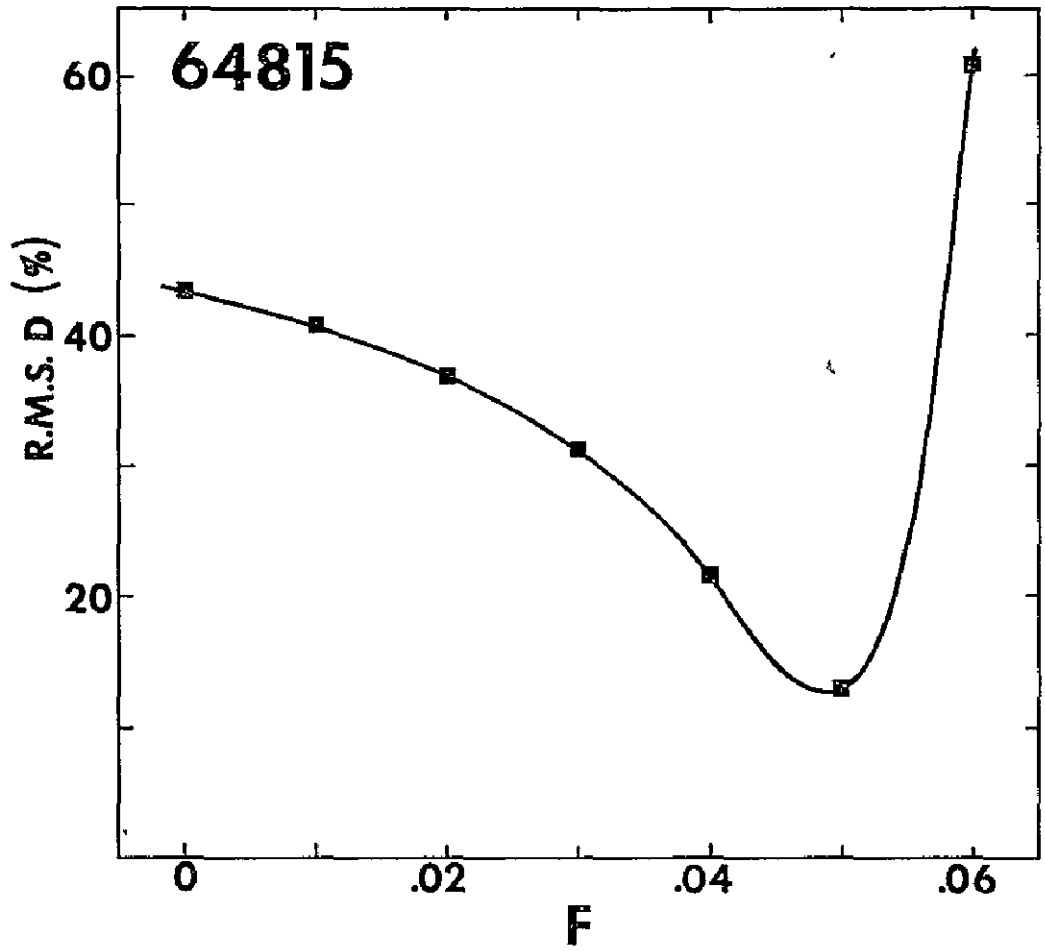

Fig 7 Quality of fit (root mean square of the percent difference between calculated and assumed $\bar{D}$ for five trace elements) of the calculated refractory mineral assemblages in equilibrium with a liquid of KREEP composition 64815 at varying degrees of melting

Table 6 The bulk compositions of olivine + orthopyroxene + plagioclase assemblages (7 × chondritic LIL abundances) which form partial melts corresponding to various KREEP samples For comparison, two estimates of the composition of the whole moon are also listed.

	64815 $F = 05$	62235 $F = 02$	65015 $F = 03$	15386 $F = 01$	Whole moon (1)	Whole moon (2)
SiO_2	46 2	45 1	46 0	43 9	44 1	42 6
Al_2O_3	10 3	9 0	9 2	7 0	8 2	8 2
FeO	7 5	8 5	8 2	12 0	10 5	10 9
MgO	31 7	32 4	31 6	33 2	31 2	30 6
CaO(3)	5 8	5 0	5 0	3 9	6 0	7 6
mg	88	87	87	83	84	83

(1) Taylor and Jakeš (1974) (2) Ganapathy and Anders (1974) All normalized to 100 wt % (3) In converting from the mineral assemblages shown in Fig. 8 to the bulk compositions listed here it was assumed that the pyroxene did not contain any CaO The low values of CaO relative to whole Moon estimates are partly attributable to this procedure

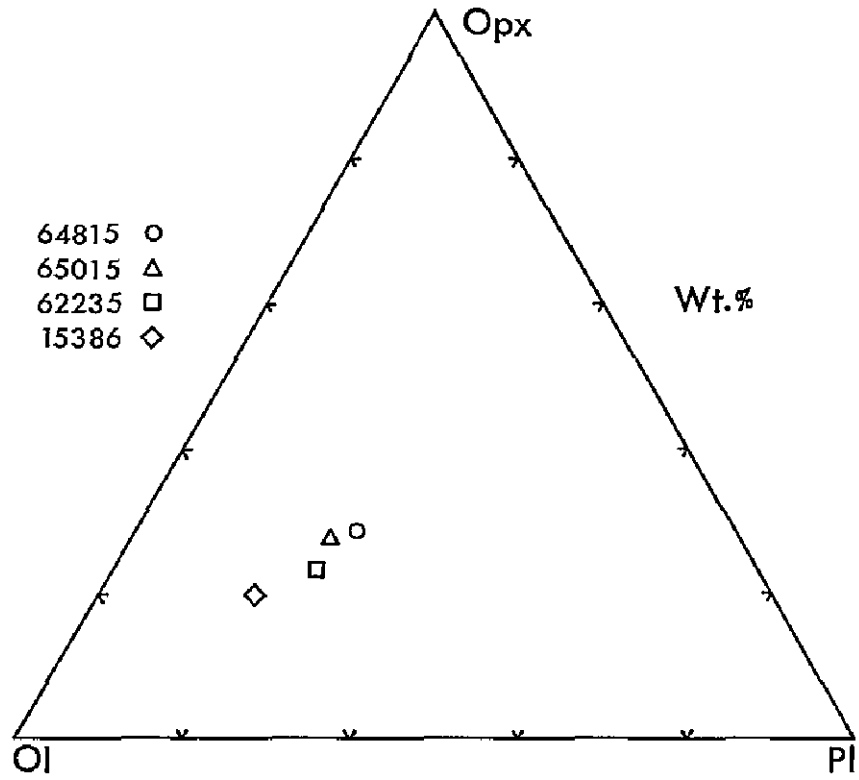

Fig 8 Refractory residual assemblages in equilibrium with four KREEP liquids LIL of bulk system is assumed to be 7× chondritic

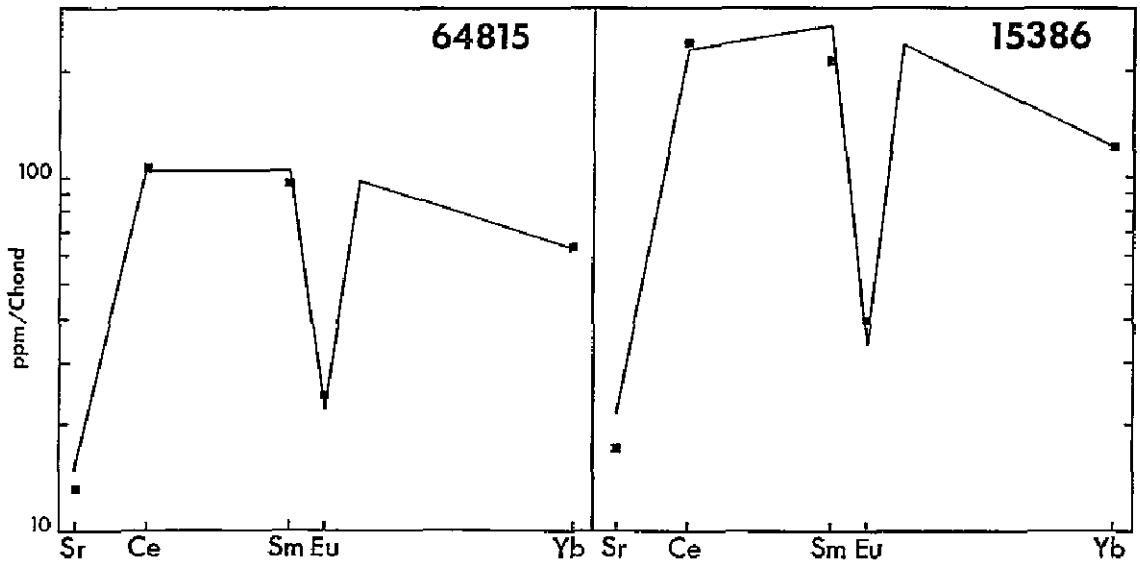

Fig 9 Comparison of calculated trace-element abundances (lines) with measured abundances (points) for KREEP samples 64815 and 15386 Liquids are in equilibrium with refractory residues whose modes are shown in Fig 8 Abundances were calculated as discussed in text, using the preferred F values indicated in Table 6

recent estimates for the whole moon In Table 6 we list the bulk composition of the parent material (refractory mineral residue plus the small fraction of KREEP melt) for each of the four preferred solutions. These are compared with two recent estimates of the whole-moon bulk composition. The agreement is not perfect, but, in view of the total range of compositions possible in the olivine–orthopyroxene–plagioclase system, we will adopt the classic stance and "stress the similarities rather than the differences " It might also be stressed that if the whole-moon composition was ever a liquid as implied in the primitive liquid shell model, then a mineral assemblage corresponding approximately to the undifferentiated composition might well be expected to occur near the surface

We have presented experimental data on phase equilibria and the partitioning of two major elements (Mg and Fe) and five trace elements (Sr, Ce, Sm, Eu, and Yb) in lunar igneous systems and have attempted to show how such a combination of data provide a powerful constraint on geochemical modeling Obviously, each element and phase added to the list will provide much greater credibility to the decreasing number of models that remain plausible. There are many elements and phases left, and we can close on an upbeat note· more work can certainly be done

Acknowledgments—Our research was supported by NASA grants NGL-38-003-020 and NGL-38-003-022 Helpful comments by J C Laul, D Lindstrom, and R Schmitt were much appreciated We are also grateful to Mr R Fletcher for maintaining our experimental and analytical facilities in excellent working order

References

Brett R (1973) The lunar crust A product of heterogeneous accretion or differentiation of a homogeneous Moon *Geochim Cosmochim Acta* **37**, 2697–2703

Drake M and Weill D F (1975) Partition of Sr, Ba, Ca, Y, Eu^{+2} and Eu^{+3} and other REE between plagioclase feldspar and magmatic liquid An experimental study *Geochim Cosmochim Acta* **38**, 689–712

Duncan A R , Erlank A J , Willis J P , and Ahrens L H (1973) Composition and inter-relationships of some Apollo 16 samples *Proc Lunar Sci Conf 4th*, p 1097–1113

Ganapathy R and Anders E (1974) Bulk compositions of the moon and earth estimated from meteorites *Proc Lunar Sci Conf 5th*, p 1181–1206

Grutzeck M , Kridelbaugh S , and Weill D (1974) The distribution of Sr and REE between diopside and silicate liquid *Geophys Res Lett* **1**, 273–275

Hubbard N J , Rhodes J , Gast P , Bansal B , Shih C , Wiesmann H , and Nyquist L (1973) Lunar rock types The role of plagioclase in non-mare and highland rock types *Proc Lunar Sci Conf 4th*, p 1297–1312

Hubbard N J , Rhodes J., Wiesmann H , Shih C , and Bansal B (1974) The chemical definition and interpretation of rock types returned from the non-mare regions of the moon *Proc Lunar Sci Conf 5th*, p 1227–1246

Mizutani H , Matsui T , and Takeuchi H (1972) Accretion process of the moon *The Moon* **4**, 476–489

Rhodes J and Hubbard N (1973) Chemistry, classification, and petrogenesis of Apollo 15 mare basalts *Proc Lunar Sci Conf 4th*, p 1127–1148

Roeder P L and Emslie R F (1970) Olivine–liquid equilibrium *Contrib Mineral Petrol* **29**, 275–289

Sun C , Williams R , and Sun Shine-Soon (1974) Distribution coefficients of Eu and Sr for plagioclase–liquid and clinopyroxene–liquid equilibria in oceanic ridge basalt An experimental study *Geochim Cosmochim Acta* **38**, 1415–1433

Taylor S and Jakeš P (1974) The geochemical evolution of the moon *Proc Lunar Sci Conf 5th*, p 1287–1305

Walker D , Longhi J , and Hays J (1972) Experimental petrology and origin of Fra Mauro rocks and soils *Proc Lunar Sci Conf 3rd*, p 797–817

Walker D , Longhi J , Grove T , Stolper E , and Hays J (1973) Experimental petrology and origin of rocks from the Descartes Highlands *Proc Lunar Sci Conf. 4th*, p 1013–1032

Warner J , Simonds C , and Phinney W (1974) Impact-induced fractionation in the lunar highlands *Proc Lunar Sci Conf 5th*, p 379–397

Weill D and Drake M (1973) Europium anomaly in plagioclase feldspar Experimental results and semiquantitative model *Science* **180**, 1059–1060

Weill D , McKay G , Kridelbaugh S , and Grutzeck M (1974) Modeling the evolution of Sm and Eu abundances during lunar igneous differentiation *Proc Lunar Sci Conf 5th*, p 1337–1352

Wiesmann H. and Hubbard N. (1975) A compilation of the lunar sample data generated by the Gast, Nyquist and Hubbard lunar sample PI-ships NASA Johnson Space Center. Unpublished manuscript

Earth and Planetary Science Letters, 28 (1975) 254–260

ELECTRICAL CONDUCTIVITY OF MAGMATIC LIQUIDS: EFFECTS OF TEMPERATURE, OXYGEN FUGACITY AND COMPOSITION

HARVE S. WAFF *

Hoffman Laboratory, Harvard University, Cambridge, Mass. (USA)

and

DANIEL F. WEILL

Department of Geology, University of Oregon, Eugene, Ore (USA)

Received July 22, 1975
Revised version received September 26, 1975

The effects of temperature, f_{O_2} and composition on the electrical conductivity of silicate liquids have been experimentally determined from 1200 to 1550°C under a range of f_{O_2} conditions sufficient to change the oxidation state of Fe from predominantly Fe^{2+} to Fe^{3+} Oxidation of ferrous to ferric iron in the melt has no measurable effect on the conductivity of melts with relatively low ratios of divalent to univalent cations. Under strongly oxidizing conditions a *minor* decrease of conductivity is detected in melts with high $\Sigma M^{2+}/\Sigma M^{+}$ ratios. It is concluded that for purposes of estimating the conductivity of magmatic liquids, f_{O_2} may be ignored to a first approximation Both univalent and divalent cation transport is involved in electrical conduction Melts relying heavily on divalent cations for conduction, i e melts with relatively large $\Sigma M^{2+}/\Sigma M^{+}$ ratios, show strong departures from Arrhenius temperature dependence with the apparent activation energies decreasing steadily as the temperature increases Conductivities dominated by the univalent cations, in melts with relatively small $\Sigma M^{2+}/\Sigma M^{+}$ ratios, show classical Arrhenius temperature dependence. These observations are discussed in terms of the general characteristics of the melt structure.

Compositional variations within the magmatic range account for much less than an order of magnitude variation in electrical conductivity at a fixed temperature This observation, combined with previous measurements of the conductivity of olivine (A. Duba, H.C Heard and R Schock, 1974) make it possible to state with reasonable confidence that melts occurring within the mantle will be more conductive by 3–4 orders of magnitude than their refractory residues. Potential applications to geothermometry are discussed

1. Introduction

Experimental measurements of electrical conduction in silicate liquids are of interest to the geoscientist for several reasons. High electrical conductivity anomalies in the mantle associated with a low seismic velocity zone are not compatible with the much lower conductivities of olivine recently measured by Duba et al. [1], and are likely to be related to the presence of a more conductive silicate liquid phase. Waff [2] considered the problem of modeling the bulk electrical conductivity of a solid + liquid mantle. A general result of this study was that if there is nearly total liquid bridging along grain boundaries or edges and if the conductivity of the liquid is much greater than that of the solid phases, the bulk conductivity is determined by the concentration of the liquid and its conductivity. Since the composition, temperature pressure and oxidation state of partial melts can be expected to vary considerably, the effect of these variables must be established before it can be assumed

* Present address: Department of Geology and Geophysics, Yale University, New Haven, Connecticut 06520.

that $\sigma_{liquid} \gg \sigma_{solid}$ under all probable mantle conditions. Such measurements also provide a direct means of studying the kinetics of ionic transport and interpreting them in terms of melt structure under controlled (T, X, f_{O_2}) conditions. Conductivity measurements can be made with high precision and are therefore potentially sensitive to physical and chemical changes in the melt.

Measurements of electrical conductivity of molten and partially molten rock systems were first reported by Barus and Iddings in 1882 [3] and have been continued until recently [4–7], among others. Analogous measurements under high confining pressure have also been reported [8–11]. None of the conductivity measurements to date have studied the effects of the oxygen fugacity or of a systematic variation of the chemical composition. These variables are known to have a strong influence on the conductivities of minerals. For example, Duba et al. [1] and Duba and Ito [12] have shown that the conductivity of olivine varies over several decades with changing Fe^{2+}/Fe^{3+} and total Fe content. We present here the results of an experimental investigation of the effects of oxygen fugacity, temperature and composition on electrical conduction in magmatic liquids.

2. Experimental technique

The rock samples listed in Table 1 were fused, quenched and ground several times to provide homogeneous starting materials. Runs were carried out while the liquids were suspended in a furnace on Pt-Rh wire circular loops bent to approximately 3.5 mm radii. The loop assemblies provided maximum surface exposure to the ambient furnace atmosphere while minimizing reaction with the container. Furnace temperature was measured with two alumina-sheathed Pt-Rh thermocouples periodically calibrated against an N.B.S. calibrated reference thermocouple and the

TABLE 1

Electron probe analyses (wt.%) of glasses quenched from post-run melts of tholeiite basalt (70-15, PG16), alkali olivine basalt (BCR2), latite (V-31) and andesite (HA). Compositions HA(2N), HA(3N), HA(3F), HA(6F) and HA(10F) correspond to base composition HA with additions of 2.1% Na_2O, 3.2% Na_2O, 3.0% FeO, 6.0% FeO and 10% FeO respectively. Total Fe is arbitrarily given as FeO.

	70-15	PG16	BCR2	V-31	HA	HA(2N)	HA(3N)	HA(3F)	HA(6F)	HA(10F)
SiO_2	47.1	47.5	53.9	61.8	57.9	57.6	57.0	57.1	55.4	53.4
TiO_2	3.03	1.54	2.58	0.79	0.63	0.63	0.62	0.62	0.60	0.58
Al_2O_3	15.2	15.1	13.3	14.2	19.0	18.9	18.6	18.7	18.2	17.5
FeO	12.2	14.6	13.3	9.1	4.99	4.96	4.90	7.83	10.4	13.7
MnO	0.21	0.13	0.02	0.15	0.09	0.09	0.09	0.09	0.09	0.08
MgO	7.58	6.91	3.57	0.38	3.10	3.08	3.05	3.05	2.97	2.86
CaO	9.5	9.8	7.5	3.50	7.7	7.6	7.5	7.5	7.33	7.06
Na_2O	2.59	2.95	3.44	4.62	4.15	6.18	7.18	4.09	3.97	3.83
K_2O	0.74	0.60	1.74	4.46	1.06	1.05	1.04	1.04	1.01	0.98
Atoms (per 100 oxygens)										
Si	29.4	29.6	32.8	36.5	33.7	33.3	33.1	33.2	32.7	32.1
Ti	1.42	0.72	1.18	0.35	0.27	0.27	0.27	0.27	0.27	0.26
Al	11.2	11.1	9.6	9.9	13.0	12.8	12.8	12.8	12.6	12.4
Fe	6.33	7.62	6.75	4.49	2.42	2.40	2.38	3.81	5.15	6.88
Mn	0.11	0.07	0.01	0.08	0.04	0.04	0.04	0.04	0.04	0.04
Mg	7.04	6.42	3.24	0.34	2.69	2.65	2.64	2.65	2.61	2.56
Ca	6.34	6.57	4.90	2.21	4.77	4.71	4.68	4.70	4.64	4.55
Na	3.13	3.57	4.06	5.29	4.67	6.93	8.08	4.61	4.54	4.46
K	0.59	0.48	1.35	3.36	0.79	0.77	0.77	0.77	0.76	0.75
Si + Ti + Al	42.0	41.4	43.6	46.7	46.9	46.4	46.1	46.3	45.6	44.8
ΣM^{2+}	19.8	20.7	14.9	7.12	9.9	9.8	9.7	11.2	12.4	14.0
ΣM^{+}	3.72	4.05	5.41	8.7	5.46	7.70	8.9	5.38	5.30	5.21

melting point of gold Uncertainties in the reported temperatures are less than ±1°C. The furnace atmosphere was controlled by mixing CO_2 and H_2 and periodically checked against a solid electrolyte oxygen cell Uncertainties in the reported oxygen fugacities are less than ±0.1 $\log_{10}$ units

For measuring resistance, the containing wire loops formed one electrode, and a centered vertical wire formed the second. Upon fusion, the sample adhered to the loop and assumed an approximately spherical shape due to surface tension. The spherical symmetry of the sample arrangement minimized the effect of volume changes when the temperature was varied and facilitated the resistance to conductivity conversion The conversion was obtained by geometric scale modeling of each sample with a liquid of known conductivity. The precision of the resistance measurements relative to each other is better than ±0.1% Resistance was measured with an AC phase-sensitive lock-in amplifier This maximized signal-to-noise ratio and eliminated unwanted polarization effects Resistances were measured from 14 to 40,000 Hz and found to be constant within ±2% over this frequency range. The values reported were taken at 2000 Hz.

3. Results

Electrical conductivities measured at 1400°C over the range of O_2 fugacities 10^{-7} to $10^{-0.7}$ atmosphere are shown in Figs. 1 and 2. The chemical compositions of the liquids are given in Table 1. Since the microprobe analyses yield only total Fe concentrations we have used wet chemistry to determine Fe^{2+} in glasses of comparable compositions that were quenched after equilibration at various temperatures and O_2 fugacities. These supporting runs indicate that at 1400°C the range of fugacities, 10^{-7} to $10^{-0.7}$ atmosphere, results in a range of $Fe^{2+}/(Fe^{2+} + Fe^{3+})$ of approximately 0.9 to 0.2 The results in Figs 1 and 2 clearly demonstrate that the conductivity is relatively insensitive to the oxidation state of Fe in the melt, and that in estimating the conductivity of liquids in the magmatic range, f_{O_2} may be ignored to a first approximation The slight decrease in conductivity observed at relatively high f_{O_2} ($>10^{-3}$ atmosphere) for compositions PG16 and BCR2 is real and is related to the higher total Fe content of these melts

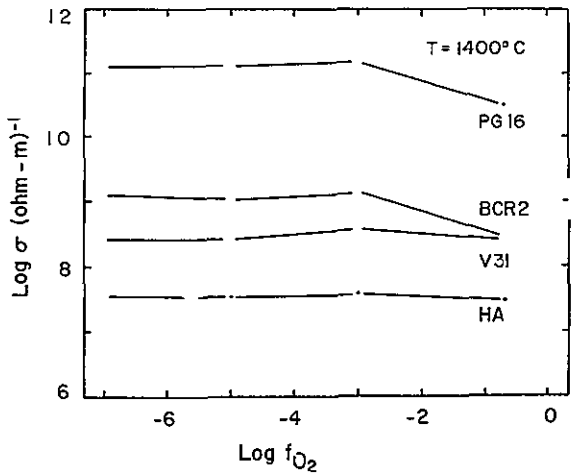

Fig 1 Electrical conductivity of melts as a function of f_{O_2} at T = 1400°C Although in detail the oxidation state of Fe in the liquid depends on the composition, it is more strongly dependent on temperature and f_{O_2} As a rough guide, $Fe^{2+}/(Fe^{2+} + Fe^{3+})$ assumes values close to 0 90, 0 75, 0 50 and 0 20 at $f_{O_2} = 10^{-7}, 10^{-5}, 10^{-3}$ and $10^{-0.7}$ respectively for the range of compositions represented in this figure and in Fig 2. Compositions are indicated in Table 1

The temperature dependence of conductivity for the various melts is shown in Figs. 3, 4 and 5 In view of the relative insensitivity of the conductivity to the oxidation state of Fe, these measurements were performed by varying the temperature while

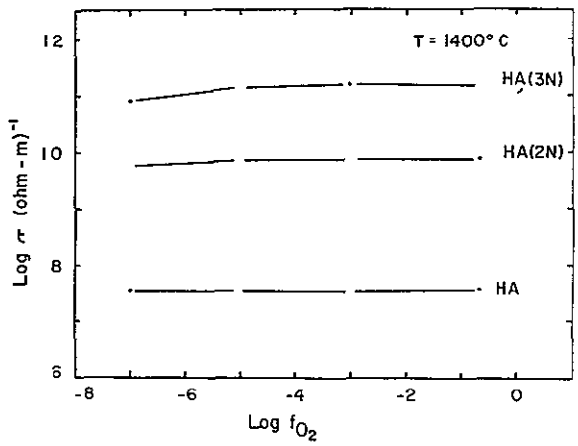

Fig 2 Electrical conductivity of andesitic melt (HA) with additions of Na_2O as a function of f_{O_2} at T = 1400°C. Compositions are indicated in Table 1

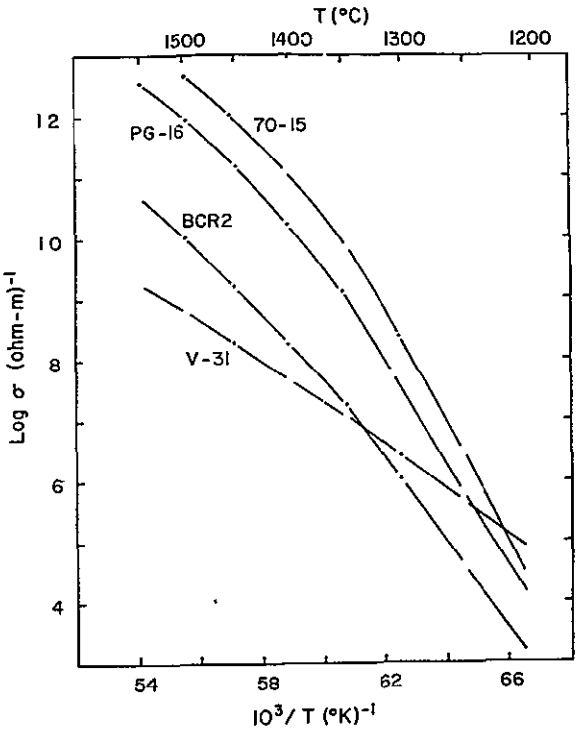

Fig 3 Electrical conductivity of melts as a function of reciprocal temperature.

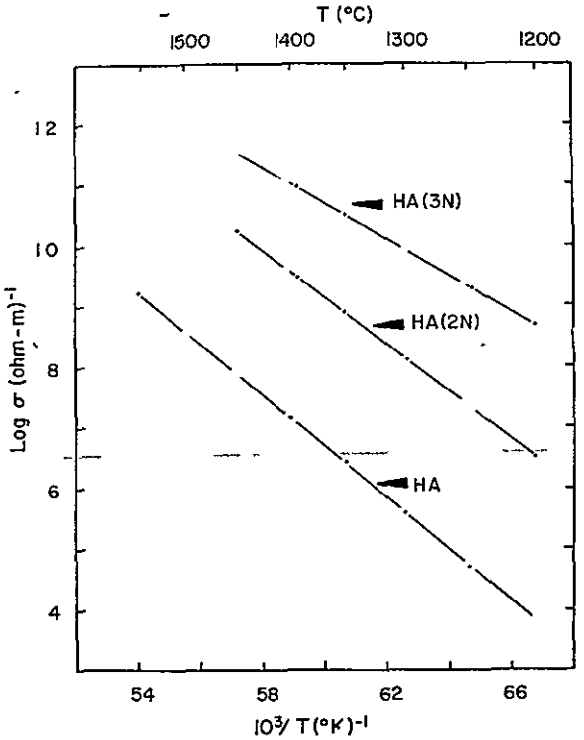

Fig 4 Electrical conductivity of andesitic melt (HA) with additions of Na_2O as a function of reciprocal temperature

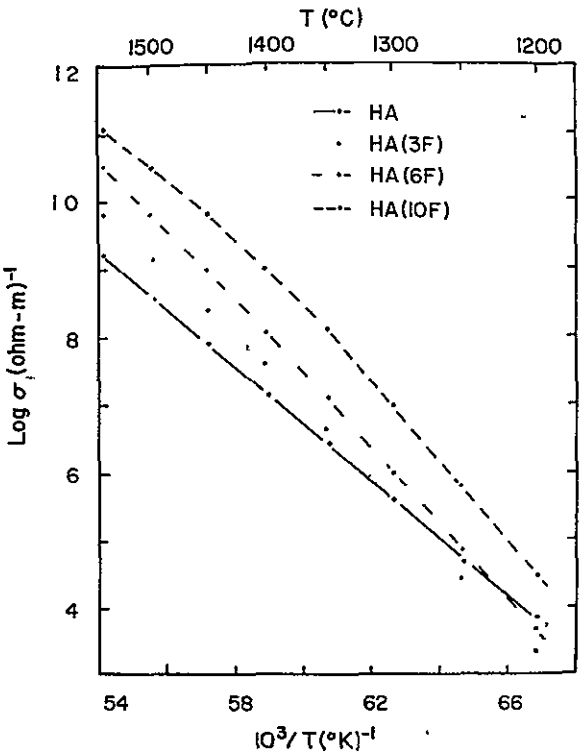

Fig 5 Electrical conductivity of andesitic melt (HA) with additions of FeO as a function of reciprocal temperature

the $CO_2/(CO_2 + H_2)$ gas mixture flowing into the furnace was held constant at 87 6% CO_2. This value of the initial composition of gas flowing into the furnace results in T–f_{O_2} conditions of 1500°–$10^{-6\,0}$, 1400°–$10^{-7\,0}$, 1300°–$10^{-8\,1}$, 1200°–$10^{-9\,3}$, and is sufficiently reducing to maintain $Fe^{2+}/(Fe^{2+} + Fe^{3+}) > 0\,90$ over the entire range of temperature During the up-down temperature cycles (50°C increments) resistance was monitored on a chart recorder and stable values were obtained within 15 minutes at each temperature Reproducibility of the data obtained during temperature cycling is excellent, typically within 1%, and the measurement and reproducibility errors in all cases are too small to display in Figs. 3, 4 and 5.

4. Discussion

Based on the following observations, we assume the electrical conductivities of these melts to be ionic in character.

(a) The measured conductivities of Na-doped andesitic melts of this study show marked and regular

increases with increasing Na concentration, a correspondence generally associated with ionic conductivity

(b) Presnall et al .[7] have demonstrated that basalt shows a rapid decrease in conductivity during the liquid-solid transition, also characteristic of ionic conduction.

(c) It has been shown that Faraday's law is obeyed in a variety of silicate glasses (cf. [13, 14]). In fact, the only reported observations of electronic conduction in glasses were for those which were fused under reducing conditions and which contain large amounts of heavy-metal ions-[14]

It should be noted that neglect of the $1/T$ dependence of the pre-exponential term in the conductivity does not alter the slopes of the log σ versus $1/T$ curves significantly over the temperature range of this study Resulting shifts in the apparent activation energies are less than 0 01 eV Thus linearity of log σ in reciprocal temperature can be properly interpreted as Arrhenius behavior.

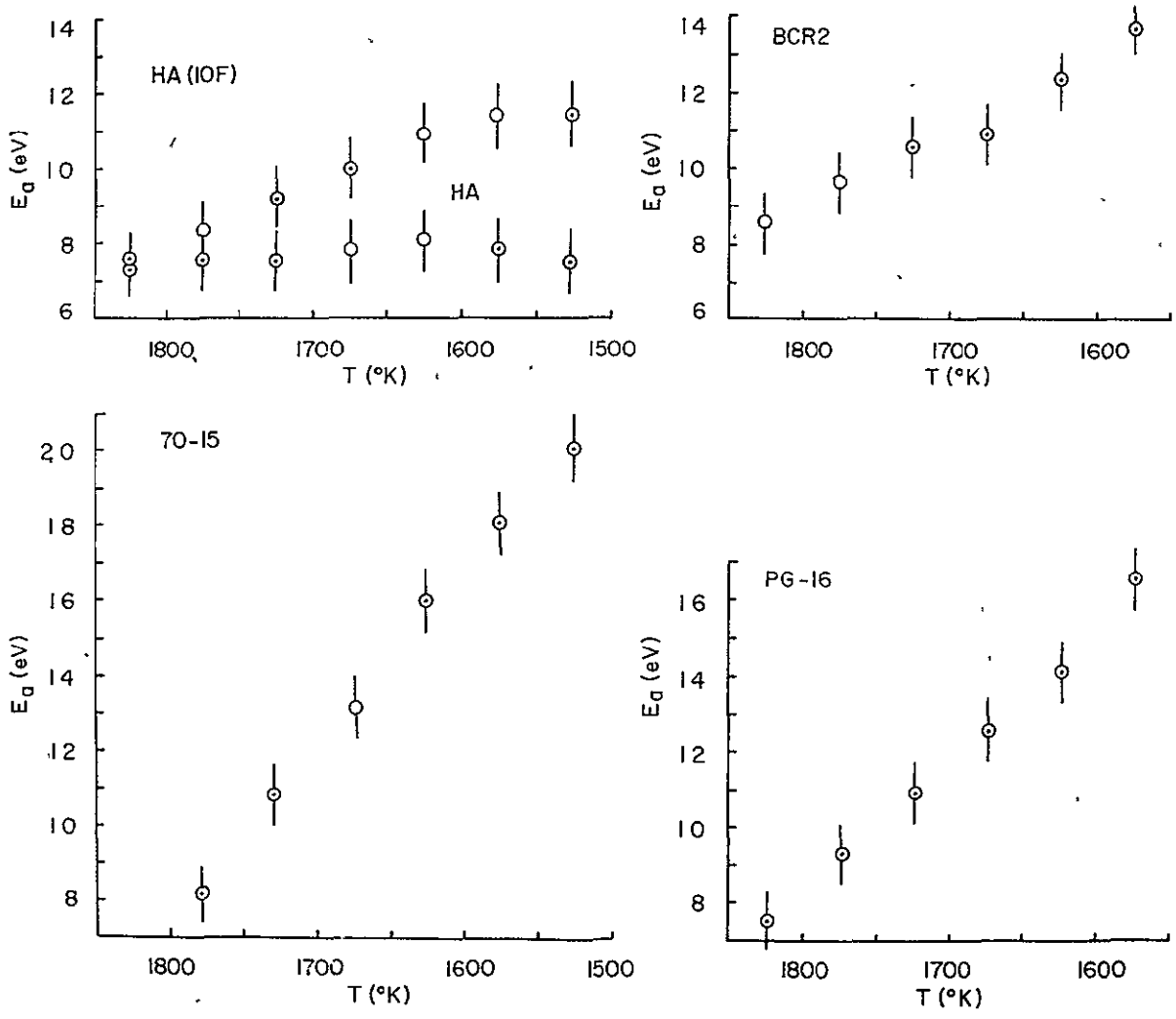

Fig. 6 Apparent activation energies for electrical conduction as a function of temperature These values were determined using conductivities measured at successive temperatures, neglecting the pre-exponential temperature dependence (see text)

Inspection of Figs 3, 4 and 5 reveals that some of the liquids show large departures from Arrhenius temperature dependence. Variations in the apparent activation energies for representative compositions are shown in Fig. 6. Compositions 70–15, PG16, BCR2 and HA(10F) show an appreciable drop in activation energy as temperature increases. Similar behavior was also found in the conductivity measurements of Presnall et al. [7] and Khitarov et al. [10]. These compositions are characterized (Table 1) by relatively high ratios of $\Sigma M^{2+}/\Sigma M^{+}$ Melts V31, HA, HA(2N) and HA(3N), with much lower $\Sigma M^{2+}/\Sigma M^{+}$ ratios, all have Arrhenius temperature dependence Silicate liquids with a high $\Sigma M^{2+}/\Sigma M^{+}$ ratio presumably depend more strongly on the divalent cations for conduction (it is assumed in this discussion that the large anionic polymer species of the silicate melt, made up mostly of SiO_4 and AlO_4 sub-units, do not contribute significantly to the conductivity) Due to their higher ionic potential (charge/radius) the divalent cations polarize the oxygens of the surrounding polymerized units in the melt structure to a greater degree than the monovalent cations. The resulting "polarization cloud" surrounding the cation must be transported along with the ion in an applied electric field This amounts to a large "effective mass" and a low mobility through the large polymerized units of the liquid structure. The divalent cations are therefore thought to be more mobile in the regions between the polymerized units than inside them. At lower temperatures the greater polymerization forces the divalent cations to migrate around the polymer species in long, tortuous paths. Hence, they are subject to increased collisions and molecular complexing probabilities per unit distance traveled parallel to the applied electric field. As the temperature is increased, thermal dissociation decreases the average size of the polymers and the volume between them increases. As a result the divalent ions can migrate along more direct paths with a consequent reduction in the apparent activation energy. Thus, the apparent activation energy for electrical conduction is expected to drop with increasing temperature in melts that have relatively high $\Sigma M^{2+}/\Sigma M^{+}$ ratios.

The monovalent cations, on the other hand, polarize the neighboring oxygens to a lesser degree and are more mobile through the polymerized units of the melt. Consequently, their path through the melt in an applied field will be less dependent upon the size and distribution of the polymerized units, and the apparent activation energies should show much less temperature dependence. This explanation is consistent with the data of Figs. 3 and 4 In addition, Hakin and Uhlmann [15], Otto and Milberg [16] and Haven and Verkerk [17] also obtained comparable activation energies down to much lower temperatures in alkali silicate glasses.

Melts with relatively large concentrations of Fe and high $\Sigma M^{2+}/\Sigma M^{+}$ ratios (hence appreciably dependent upon divalent cations for conduction) show a decrease of conductivity as the Fe^{2+}/Fe^{3+} ratio decreases (cf Fig. 1). Several reasons can be offered to explain this observation. First, a melt with more Fe^{3+} contains fewer Fe ions free to participate in conduction. This is simply related to the Boltzmann distribution of free charge carriers in the melt. Iron-oxygen binding energies are greater for Fe^{3+} than for Fe^{2+} Boon and Fyfe [18] and Waff et al [19] find that Fe^{2+} occurs only in six-fold oxygen coordination while Fe^{3+} Mossbauer spectra show isomer shifts characteristic of tetrahedral coordination in glasses quenched from natural silicate liquids. The 2+ charge on the ferrous ion is shared among six nearest-neighbor oxygens. Ferric iron, on the other hand, shares a charge of 3+ among either four or six oxygens and therefore has from 1/6 to 5/12 greater charge per Fe–O bond. A smaller fraction of ferric ions will be disassociated at any given temperature than ferrous ions Second, an increase of Fe^{3+} ions in FeO_4 tetrahedral sites may reduce the effective number of univalent and divalent cations that can participate in conduction The main polymerizing sub-units of the melt, SiO_4^{-4} can be replaced by AlO_4^{-5} or FeO_4^{-5} only if M^{+} or M^{2+} cations are available to locally offset the charge imbalance from substituting Al^{3+} or Fe^{3+} for Si^{4+} This charge balancing role for M^{+} and M^{2+} ions (analogous to their role in the feldspar structures) ties up a fraction of these ions and effectively reduces their overall mobility

Perhaps the most obvious and significant result of these measurements is that the total range of magmatic compositions and temperatures (approximately 1200–1550°C) studied here accounts for less than an order of magnitude change in the conductivity. This means that the conductivity differences to be expected between liquids of magmatic compositional extremes will always be much less than those between solids

(e g., olivine) and liquid silicates In the melting range of temperatures postulated for the mantle, the partial melt will always be more conductive by a factor of 2–4 decades. As discussed by Waff [2], it is probable that under these conditions a relatively small amount of partial melt can dominate the bulk conductivity Furthermore, a comparison of conductivities among the less differentiated compositions studied here (e.g., 70–15 and PG16) and comparable compositions under very different conditions of confining pressure, and H_2O and O_2 fugacities in earlier studies [7,8,10,11] strongly suggests that within this compositional grouping the temperature dependence is dominant. If so, it should be possible to convert geomagnetic depth-soundings to geothermometry of deep-seated magma sources Conductivity profiles should at the very least be able to tell us whether we are dealing essentially with a solid or partially melted material, i.e , whether or not we are in the temperature range above the solidus If we can make a reasonable assumption about the gross compositional characteristics of the partial melt, it may additionally be possible to estimate temperatures more precisely

Acknowledgments

Our research was supported by NASA grant NGL 38-003-202 Thanks are expressed to Michael Grutzeck for his assistance with construction of the apparatus and in data acquisition We are grateful to Richard Stocker for a critical review of the paper.

References

1 A Duba, H C Heard and R Schock, Electrical conductivity of olivine at high pressure and under controlled oxygen fugacity, J Geophys Res 79 (1974) 1667–1673
2 H S Waff, Theoretical considerations of electrical conductivity in a partially molten mantle and implications for geothermometry, J Geophys Res 79 (1974) 4003–4010
3 C Barus and J P Iddings, Note on the change of electrical conductivity in rock magmas of different composition on passing from liquid to solid, Am J. Sci , 3rd Ser. 44 (1892) 242–249.
4 M P. Volarovich and D M Tolstoi, The simultaneous measurement of viscosity and electrical conductivity of some fused silicates at temperatures up to 1400°, Soc Glass Tech J 20 (1936) 54–60
5 T Nagata, Some physical properties of the lava of volcanoes, Asama and Mihara, Bull Earthquake Res Inst Japan 15 (1937) 663–673.
6 T Murase, Viscosity and related properties of volcanic rocks at 800 to 1400°C, J Fac Sci Hokkaido Univ , Ser 7, 1 (1962) 487–584
7 D C Presnall, C L Simmons and H Porath, Changes in electrical conductivity of a synthetic basalt during melting, J Geophys Res 77 (1972) 5665–5671
8 E B Labedev and N I Khitarov, Dependence of the beginning of melting of granite and the electrical conductivity of its melt on high vapor pressure, Geochem Int 1 (1964) 193–197
9 N I Khitarov and A B Slutskiy, The effect of pressure on the melting temperatures of albite and basalt, Geochem Int 2 (1965) 1034–1041
10 N I Khitarov, A B Slutskiy and V A Pugin, Electrical conductivity of basalts at high T–P and phase transitions under upper mantle conditions, Phys Earth Planet Inter 3 (1970) 334–342
11 H Watanabe, Measurements of electrical conductivity of basalt at temperatures up to 1500°C and pressures to about 20 kilobars, Spec Contrib , Geophys Inst , Kyoto University 10 (1970) 159–170
12 A Duba and J Ito, The effect of ferric iron on the electrical conductivity of olivine, Earth Planet Sci Lett 18 (1973) 279–284
13 J E Stanworth, Physical properties of glass (Oxford, 1950) 124–126
14 W Eitel, The Physical Chemistry of the Silicates (Univ of Chicago Press, 1954) 205–206, and 1346
15 R M Hakin and D R Uhlmann, Electrical conductivity of alkaline silicate glasses, Phys Chem Glasses 12 (1973) 132–138
16 K. Otto and M E Milberg, Ionic conduction in alkali and thallium silicate glasses, J Am. Ceramic Soc 51 (1968) 326–329
17 Y Haven and B Verkerk, Diffusion and conductivity of sodium ions in sodium silicate glasses, Phys Chem Glasses 6 (1965) 38–45.
18 J.A Boon and W S Fyfe, Mossbauer investigations in the system Na_2O–FeO–SiO_2, Chem Geol. 7 (1971) 153–169.
19 H.S Waff, H H Wickmann and D.F Weill, Mössbauer spectra of silicate glasses evidence for chemically induced coordination changes of ferric iron, unpublished.

ABSTRACTS

McKAY, G. A. and D. F. Weill (1976) Petrogenesis of KREEP. Proc. Lunar Sci. Conf. 7th, in press.

Abstract - Solid/liquid distribution coefficients (weight basis) have been experimentally determined for a number of trace elements for olivine, orthopyroxene, plagioclase and ilmenite. Values of distribution coefficients measured at 1200°C and f_{O_2} of $10^{-13.0}$ for liquids similar in composition to the olivine-opx-plagioclase peritectic in the pseudoternary system $(Fe,Mg)_2SiO_4$-$CaAl_2Si_2O_8$-SiO_2 are as follows: olivine: Ce = 0.010±.007, Sm = 0.015±.005, Eu = 0.015±.005, Yb = 0.033±.002, Cr = 1.2±.1; orthopyroxene: Ba = 0.011±.005, Cr = 5.2±.2; anorthite: Rb = 0.017±.008, Ba = 0.15±.03. Values measured at 1140°C and f_{O_2} of $10^{-12.8}$ for liquids similar in composition to high-Ti mare basalts are as follows: ilmenite: Ce = 0.006±.003, Sm = 0.010±.002, Yb = 0.075±.005. Cr distribution coefficients decrease with decreasing oxygen fugacity for both pyroxene and olivine, but are larger for pyroxene than for olivine at all fugacities investigated. The variation of D_{Cr} with oxygen fugacity indicates that a substantial fraction of the Cr is divalent at lunar oxygen fugacities.

Major and trace element partitioning and relevant phase equilibria are used to investigate possible parent-daughter relationships between a number of highland samples and highly evolved KREEP-rich materials. Out of about 80 highland samples tested, 33 are found to be possible parents to the KREEP-rich materials. The average composition of these 33 samples is very similar to that of the Low-K Fra Mauro basalt (LKFM). A model is proposed in which LKFM-type material was produced by fractionation of large amounts of olivine and lesser amounts of plagioclase (and possibly other minor phases) from undifferentiated lunar material at ∿4.4 AE. During the same episode of igneous activity, some LKFM material differentiated to form a series of more evolved members of the KREEP suite, including material of peritectic bulk composition in the $(Mg,Fe)_2SiO_4$-$CaAl_2Si_2O_8$-SiO_2 pseudoternary system. In a later igneous event at ∿3.9 AE, some of this peritectic material further differentiated, producing more highly evolved KREEP such as sample 15386. The model is consistent with phase equilibria, major and trace element partitioning, and Rb-Sr isotopic data.

LINDSTROM, D. J. (1976) Experimental Study of the Partitioning of the Transition Metals Between Clinopyroxene and Coexisting Silicate Liquids. Ph.D. thesis, University of Oregon.

Abstract - This study describes the partitioning of the transition elements Sc, Ti, V, Cr, Mn, Fe, Co, and Ni between silicate liquids and coexisting crystalline phases (emphasizing clinopyroxene but also including low-Ca pyroxene, olivine, plagioclase, magnetite, and pseudobrookite).

Equilibration experiments were preformed at one atmosphere total pressure, mixtures of H_2 and CO_2 being used to control oxygen fugacity. Temperatures ranged from 1110 to 1340°C. Bulk compositions were largely chosen from the system $MgCaSi_2O_6$-$NaLiSi_3O_8$-$CaAl_2Si_2O_8$. Aliquants were doped with a few percent transition metal oxide. Experiments were also run on a natural basaltic composition. Quenched phases were analyzed with the electron microprobe.

The crystal/liquid distribution coefficients are independent of the transition metal content. Analyses of pyroxenes grown from liquids with varying concentrations of transition metal ions present indicated the types of cation substitutions on the pyroxene lattice. Except for Mn^{2+} and Ti^{4+}, all species studied appear to substitute primarily in the M1 (Mg) site of clinopyroxene.

Weight ratio distribution coefficients, D_i, exhibit considerable compositional dependence, particularly between the synthetic compositions chosen and the basalt.

When equilibrium constants are calculated according to the model of Bottinga and Weill (1972), the compositional dependence disappears. Activities of cations in the liquid are approximated by their concentrations relative to the silicate melt network forming or network modifying components, e.g.,

$$a_{Si} \simeq X_{Si} = \frac{N_{Si}}{N_{Si} + N_{Ti} + N_{KAl} + N_{NaAl} + 2N_{CaAl_2}}$$

$$a_{Ni} \simeq X_{Ni} = \frac{N_{Ni}}{N_{Ni} + (N_{Ca} - N_{CaAl_2}) + N_{Mg} + N_{Fe} + \ldots\ldots}$$

These mole fractions are combined in the equilibrium constant for the reaction forming the pyroxene component, e.g.,

$$NiO_{liq} + CaO_{liq} + 2SiO_{2\ liq} = (NiCaSi_2O_6)_{pyx}$$

$$K_{Ni}^{pyx} = \frac{X_{NiCaSi_2O_6}^{pyx}}{X_{Ni}^{liq}\ X_{Ca}^{liq}\ (X_{Si}^{liq})^2}$$

where the activity of $NiCaSi_2O_6$ is taken to be the mole fraction of Ni on the M1 site.

Values for D_i for clinopyroxene are in the order $Cr^{3+}>V^{3+}>Ni^{2+}>Mg^{2+}>Sc^{3+}>Co^{2+}>Fe^{2+}\sim Fe^{3+}\sim Mn^{2+}>Ti^{4+}>V^{5+}(?)$.

When Sc^{3+} enters the M1 site of clinopyroxene, the charge balance is maintained by the simultaneous replacement of Na^{+} for Ca^{2+} in the M2 site or Al^{3+} for Si^{4+} in a tetrahedral site. The existence of the two independent reactions precludes the use of a simple equilibrium constant to describe the partitioning.

Chromium enters pyroxene in a similar fashion, but the very limited solubility of Cr^{3+} in the liquid presents serious experimental difficulties so that the D values are only approximate.

Vanadium exists in at least two oxidation states. V^{3+} predominates at low oxygen fugacities near the iron/wüstite buffer. In air, the observed D drops by two orders of magnitude to as low as 0.04, suggesting that V^{5+} may be present. V^{4+} is by no means ruled out, however.

Ti^{4+} enters both tetrahedral and octahedral sites in the pyroxene, octahedral sites being somewhat favored.

Mn^{2+} enters both the M1 and M2 sites, apparently in near equal amounts. Detailed modeling requires data on intracrystalline distributions not available from microprobe analyses.

At the low doping levels (usually 2% Fe) used in these experiments, Fe^{2+} and Fe^{3+} enter clinopyroxene with equal ease.

Co^{2+} and Ni^{2+} behave similarly; both can be described by the equilibrium constants discussed above.

A few data on low-Ca pyroxenes are reported. Observed D's for the divalent ions are higher than those of clinopyroxenes while D's for trivalent and quadrivalent ions are lower.

Similar trends are apparent in the olivine data. Partitioning of the divalent ions is adequately described as

$$NiO_{liq} + 1/2\ SiO_{2\ liq} = (NiSi_{0.5}O_2)_{olivine}$$

$$K = \frac{X_{NiSi_{0.5}O_2}^{ol}}{X_{Ni}^{liq}\ (X_{Si}^{liq})^{1/2}}$$

A few data on plagioclases show that the transition elements are rather strongly excluded except for Fe^{3+}.

Fe-Ti oxide minerals strongly take up the transition elements, Sc and the quadrivalent ions being preferentially incorporated in pseudobrookite while the other ions discriminate in favor of magnetite.

WAFF, H. S. and D. F. WEILL (1975) Electrical Conductivity of Magmatic Liquids: Effects of Temperature, Oxygen Fugacity and Composition. Earth Planet. Sci. Lett., 28, 254-260.

Abstract - The effects of temperature, f_{O_2} and composition on the electrical conductivity of silicate liquids have been experimentally determined from 1200 to 1550°C under a range of f_{O_2} conditions sufficient to change the oxidation state of Fe from predominantly Fe^{2+} to Fe^{3+}. Oxidation of ferrous to ferric iron in the melt has no measurable effect on the conductivity of melts with relatively low ratios of divalent to univalent cations. Under strongly oxidizing conditions a *minor* decrease of conductivity is detected in melts with high $\Sigma M^{2+}/\Sigma M^{+}$ ratios. It is concluded that for purposes of estimating the conductivity of magmatic liquids, f_{O_2} may be ignored to a first approximation. Both univalent and divalent cation transport is involved in electrical conduction. Melts relying heavily on divalent cations for conduction, i.e. melts with relatively large $\Sigma M^{2+}/\Sigma M^{+}$ ratios, show strong departures from Arrhenius temperature dependence with the apparent activation energies decreasing steadily as the temperature increases. Conductivities dominated by the univalent cations, in melts with relatively small $\Sigma M^{2+}/\Sigma M^{+}$ ratios, show classical Arrhenius temperature dependence. These observations are discussed in terms of the general characteristics of the melt structure.

Compositional variations within the magmatic range account for much less than an order of magnitude variation in electrical conductivity at a fixed temperature. This observation, combined with previous measurements of the conductivity of olivine (A.Duba, H.C.Heard and R.Schock, 1974)make it possible to state with reasonable confidence that melts occurring within the mantle will be more conductive by 3-4 orders of magnitude than their refractory residues. Potential applications to geothermometry are discussed.

LEEMAN, W. P. (1974) Experimental Determination of Partitioning of Divalent Cations Between Olivine and Basaltic Liquid. Ph.D. thesis, University of Oregon.

Abstract - The distribution of divalent Ni, Mg, Co, Fe, Mn, and Ca between olivine and natural basaltic liquid was investigated between 1070°C and 1400°C. Relative magnitudes of the distribution coefficients decrease in the order listed above. Distribution coefficients defined as the ratio of weight fractions (D) or the theoretical equilibrium constant (K) are strongly temperature dependent for all of these elements. Compound distribution coefficients (e.g., $K_{Ni/Mg}$) are less temperature dependent. Linear regression equations, ln D (or K) = A/T + B, are given for each element. These equations may be used as geothermometers to obtain olivine crystallization temperatures. Applications to experimental runs and natural volcanic rocks suggest that under optimum conditions temperatures can be estimated with an accuracy of better than ±30°. Simple D values are apparently not very sensitive to differences in bulk composition within the range of terrestrial basalt. Temperature calibrations of D may be useful in constructing detailed crystallization or melting models involving olivine.

WEILL, D. F. and G. A. McKAY (1975) The partitioning of Mg, Fe, Sr, Ce, Sm, Eu, and Yb in Lunar Igneous Systems and a Possible Origin of KREEP by Equilibrium Partial Melting. Proc. Lunar Sci. Conf. 6th, 1143-1158.

Abstract - The solid/liquid distribution of Mg, Fe, Sr, Ce, Sm, Eu, and Yb have been determined over crystallization paths in the system $(Mg,Fe)_2SiO_4$-$CaAl_2Si_2O_8$-SiO_2. Varying degrees (1-5 wt.%) of partial melting of an olivine + orthopyroxene + plagioclase rock yield liquids with large-ion lithophile (LIL) and major-element concentrations strikingly similar to those of some Apollo 15 and 16 KREEP rocks. The parent assemblages from which these KREEP melts can be derived have a bulk composition similar to that previously proposed for the whole moon. Partial melts derived from a source with the same mineralogy but with a chemical composition corresponding to the average lunar highlands do not simultaneously satisfy the major-element and LIL concentration characteristics of KREEP.

WEILL, D. F., MCKAY, G. A., KRIDELBAUGH, S. J. and M. GRUTZECK (1974) Modeling the Evolution of Sm and Eu Abundances During Lunar Igneous Differentiation. Geochim. Cosmochim. Acta, Suppl. 5, vol. 2, 1337-1352.

Abstract - Models are presented for the evolution of Eu and Sm abundances during lunar igneous processes. The effect of probable variations in lunar temperature and oxygen fugacity, mineral-liquid distribution coefficients, and the crystallization or melting progression are considered in the model calculations. Changes in the proportions of crystallizing phases strongly influence the evolution of trace element abundances during fractional crystallization, and models must include realistic estimates of the major phase equilibria during crystallization.

The results are applied to evaluate the possibility of generating KREEP-rich materials by lunar igneous processes. Fractional crystallization of a primordial liquid shell is a very unlikely origin because the characteristic Sm and Sm/Eu abundances of KREEP are achieved only after a very high degree of fractionation involving separation of mostly ferromagnesian minerals. The low Fe/Mg found in KREEP is incompatible with such a history. All fractional crystallization sequences involving appreciable separation of plagioclase produce negative Eu anomalies that are much too large.

Partial melting of olivine-orthopyroxene-clinopyroxene-plagioclase assemblages can produce KREEP abundances of Sm and Sm/Eu. The most probable parent assemblages are (1) dominantly olivine plus orthopyroxene (<20% plagioclase and a few percent clinopyroxene) with bulk Sm and Sm/Eu concentrations comparable to those estimated for the whole moon; i.e. enriched approximately tenfold or less relative to chondrites, with no Eu anomaly, or (2) a rock with more plagioclase, enriched in both Sm and Eu (no negative Eu anomaly) relative to the whole moon. An origin for either of these parental bulk compositions via fractional crystallization implies a low concentration of plagioclase constituent relative to ferromagnesian constituents in the moon's primordial liquid shell.

Although the range of Sm and Sm/Eu abundances may be related to varying degrees of partial melting of these parental assemblages, it is also possible that the variation may simply reflect different amounts of olivine plus orthopyroxene relative to plagioclase plus clinopyroxene in the parent material.

DRAKE, M. J. (1975) The oxidation state of europium as an indicator of oxygen fugacity. Geochim. Cosmochim. Acta, 39, 55-64.

Abstract - The distribution of Eu between plagioclase feldspar and magmatic liquid has been determined experimentally for basaltic and andesitic systems as a function of temperature and oxygen fugacity at one atmosphere total pressure. Using the approach of Philpotts, the ratios Eu^{2+}/Eu^{3+} in plagioclase and coexisting magmatic liquid have been calculated. These ratios

appear to be simply related to oxygen fugacity for the bulk compositions studied here. Using published trace element distribution data for natural rocks, oxygen fugacities may be calculated from these experimental results. For terrestrial basalts, calculated oxygen fugacities average 10^{-7} with little dispersion from this value. Andesites average $10^{-8.1}$ with considerable dispersion, while dacites and rhyodacites average $10^{-9.1}$, also with considerable dispersion. Oxygen fugacities for lunar ferrobasalts cluster tightly around $10^{-12.7}$. Data on achondritic meteorites are limited, but calculations indicate oxygen fugacities of two-to-five orders of magnitude lower than lunar ferrobasalts.

DUNCAN, A. R., GRIEVE, R. A. and D. F. WEILL (1975) The life and times of Big Bertha: lunar polymict breccia 14321. Geochim. Cosmochim. Acta, 39, 265-273.

Abstract - The lithic units of polymict breccia 14321 (Big Bertha) have been grouped according to composition, texture, degree of metamorphism, and additional criteria based on a systematic study of the interrelationships of all clast-matrix pairs. From this information it has been possible to reconstruct the assembly and metamorphic history of this breccia. The earliest formed fragmental component of 14321 (microbreccia-1) is dominated by KREEP-rich norite, extruded and subsequently brecciated and lithified in an ejecta blanket at approximately 1000°C in the general region of Mare Imbrium after the Serenitatis impact but prior to the Imbrium impact. This early microbreccia component and lesser amounts of mare-type basalt, microgranite, rhyolite glass, anorthosite and olivine microbreccia were assembled at the Apollo 14 site as part of the Fra Mauro ejecta blanket from the Imbrium impact. The resulting microbreccia-3 incorporates all the lithic types above and accretionary lapilli structures (microbreccia-2) in a dark matrix annealed at approximately 700°C. A later impact on the Fra Mauro excavated and mutually abraded microbreccia-3 and a local, 14321-type, basalt which were assembled into polymict breccia 14321. Final placement of 14321 at its sampling location was accomplished during the minor Cone Crater impact event.

GRIEVE, R., MCKAY, G., SMITH, H. and D. F. WEILL (1975) Lunar polymict breccia 14321: a petrographic study. Geochim. Cosmochim. Acta, 39, 229-245.

Abstract - The lithic units of polymict breccia 14321 (Big Bertha) have been grouped according to composition, texture, degree of metamorphism, and additional criteria based on a systematic study of the interrelationships of all clast-matrix pairs. From this information it has been possible to reconstruct the assembly and metamorphic history of this breccia. The earliest formed fragmental component of 14321 (microbreccia-1) is dominated by KREEP-rich norite, extruded and subsequently brecciated and lithified in an ejecta blanket at approximately 1000°C in the general region of Mare Imbrium after the

Serenitatis impact but prior to the Imbrium impact. This early microbreccia component and lesser amounts of mare-type basalt, microgranite, rhyolite glass, anorthosite and olivine microbreccia were assembled at the Apollo 14 site as part of the Fra Mauro ejecta blanket from the Imbrium impact. The resulting microbreccia-3 incorporates all the lithic types above and accretionary lapilli structures (microbreccia-2) in a dark matrix annealed at approximately 700°C. A later impact on the Fra Mauro excavated and mutually abraded microbreccia-3 and a local, 14321-type, basalt which were assembled into polymict breccia 14321. Final placement of 14321 at its sampling location was accomplished during the minor Cone Crater impact event.

DRAKE, M. J. and D. F. WEILL (1975) Partition of Sr, Ba, Ca, Y, Eu^{2+} and Eu^{3+} and other REE between plagioclase feldspar and magmatic liquid: an experimental study. Geochim. Cosmochim. Acta, in press.

Abstract - Plagioclase feldspar/magmatic liquid partition coefficients for Sr, Ba, Ca, Y, Eu^{2+}, Eu^{3+} and other REE have been determined experimentally at one atmosphere total pressure in the temperature range 1150-1400°C. Natural and synthetic melts representative of basaltic and andesitic bulk compositions were used, crystallizing plagioclase feldspar in the composition range An_{35} to An_{85}. Partition coefficients for Sr are greater than unity at all geologically reasonable temperatures, and for Ba are less than unity above approximately 1060°C. Both are strongly dependent upon temperature. Partition coefficients for the trivalent REE are relatively insensitive to temperature. At fixed temperature they decrease monotonically from La to Lu. The partition of Eu is a strong function of oxygen fugacity. Under extreme reducing conditions D_{Eu} approaches the value of D_{Sr}.

GRUTZECK, M., KRIDELBAUGH, S. and D. F. WEILL (1974) The distribution of Sr and REE between diopside and silicate liquid. Geophys. Res. Letters, 1, 273-275.

Abstract - Distribution coefficients (weight concentration in the solid divided by concentration in the liquid) have been determined experimentally in diopside-liquid pairs. Experiments were carried out in air at 1265°C in the system $NaAlSi_3O_8$-$CaAl_2Si_2O_8$-$CaMgSi_2O_6$ at the two bulk compositions: 5-30-65 and 32-11-57 (weight percentage of components in the order given above). Small differences are observed in the distribution coefficients between the two compositions. Mean values of the coefficients in the first system are: Sr=.078, La=.069, Ce=.098, Nd=.21, Sm=.26, Eu=.31, Gd=.30, Dy=.33, Er=.30 and Lu=.28. At low oxygen fugacities of $10^{-9.5}$ and $10^{-12.5}$ atmospheres the distribution of Eu between diopside and liquid develops a "negative Eu-anomaly" with coefficients of .23 and .12 respectively.

SMITH, H. D. (1973) An Experimental Study of the Diffusion of Na, K, and Rb in Magmatic Silicate Liquids. Ph.D. thesis, University of Oregon.

Abstract - In this study an experimental method was developed for the determination of diffusion coefficients in multicomponent silicate melts. This method was then applied to the study of the diffusion of Na^+, K^+, and Rb^+ in three silicate melts which were modeled compositionally after a basalt, an andesite, and a rhyolite.

Diffusion in a multicomponent system is described generally by a "diffusion matrix" [see Onsager (1945), Cooper (1965)]. However, subject to certain limitations, a single coefficient can be used to describe the diffusion of a single component through a liquid of given composition. This coefficient is the Effective Binary Diffusion Coefficient, EBDC, described by Cooper (1968).

In this study the EBDCs for Na^+, K^+, and Rb^+ were determined by setting up diffusion couples in which concentration gradients were present only for the alkalies. Cylinders of melt with the same base melt composition but containing different alkalies were joined end-to-end and diffusion allowed to take place. After quenching, each couple was sectioned lengthwise and an electron microprobe was employed to determine the concentration profiles that developed for each alkali. From these concentration profiles it was possible to determine the EBDC at regular intervals along the profile by graphical application of the Boltzmann-Matano analysis. The D_is (EBDC) so determined cover a wide range of temperature (1128°C to 1535°C) and compositional variables.

The findings of this experimental study can be summarized as follows: 1) Strong electrical coupling between ionic fluxes is indicated by the near equality of opposed alkali fluxes in most couples. A measurable amount of "uphill diffusion" of calcium in some couples of basaltic and andesitic (calcium-rich) compositions also demonstrates the ability of other relatively mobile ions to participate in ionic exchange diffusion within silicate melt structures. 2) D_i varies with position along the concentration profile of i (conveniently represented by the ratio $\omega_i \equiv C_i - C_1 / C_2 - C_1$ in which C_i is the concentration of i and C_1 and C_2 are the concentrations at the ends of the effectively infinite couple). For example, there is a factor of 20 variation for D_{Rb} and D_{Na} between $\omega = 0$ and $\omega = 1$ in Rb-Na-rhyolite couples. In contrast, D_{Rb} and D_K exhibit very little variation across the Rb-K-basalt couples. These two examples represent the extreme cases found in this study. Comparisons of the diffusion coefficients of the alkalies for the purpose of evaluating the effects of temperatures or matrix composition must be made at comparable ω values ($\omega = \frac{1}{2}$ in this study). 3) The D_i (EBDC) values are Arrhenius functions within the range of temperature used in this study. The apparent activation energies, E_i, vary from 26 Kcal/mole for D_{Na} in K-Na-rhyolite to 48 Kcal/mole for D_{Rb} in Rb-K-basalt systems. 4) E_i^{Na} varies systematically with the liquid matrix composition. A linear relationship was found between E_i and the percentage of silicate network forming (NWF) units in the liquid for each ion pair (Rb-Na, K-Na, Rb-K). E_i decreases with increasing NWF percentage. 5) Analysis of E_i and D_i° via absolute rate theory suggests that rhyolite compositions form open structured melts while basalt compositions form relatively compact-structured melts. The concurrent

variation of E_i and D_i^o (the "Compensation" effect) is in full agreement with that shown by diffusion data in other silicate systems [see Winchell (1969)]. 6) Basalt-andesite mixed couples demonstrate that the D_is for the alkalies are much larger (about 30 times) when exchange between different alkalies can occur. When only one alkali is present in a couple, the D_is for all the elements are about the same magnitude.

In the final section, three cases of diffusion in natural systems are analysed, two of lunar and one of terrestrial origin.

WEILL, D. F. and M. J. DRAKE (1973) Europium Anomaly in Plagioclase: Experimental Results and Semiquantitative Model. Science, 180, 1059-1060.

Abstract - The partition of europium between plagioclase feldspar and magmatic liquid is considered in terms of the distribution coefficients for divalent and trivalent europium. A model equation is derived giving the europium anomaly in plagioclase as a function of temperature and oxygen fugacity. The model explains europium anomalies in plagioclase synthesized under controlled laboratory conditions as well as the variations of the anomaly observed in natural terrestrial and extraterrestrial igneous rocks.